EPRI-VOID MODEL

# A Mechanistic Model

# for

# Predicting Two-Phase Void Fraction for Water

# in

# Vertical Tubes, Channels, and Rod Bundles

by

G. S. Lellouche

B. A. Zolotar

## Nomenclature

| | | |
|---|---|---|
| $\left(\frac{A}{V}\right)_c$ | = ratio of bubble area to bubble unit cell volume | $ft.^{-1}$ |
| $C_o$ | = Distribution Coefficient with slip relation | |
| $c_{1,2}$ | = Constant in the slip relation | |
| $C_E$ | = Proportionality constant in bulk evaporation coefficient | |
| $C_A$ | = Proportionality constant in the Hancox-Nicol relation | |
| $C_D$ | = Proportionality constant in the Dittus-Boelter relation | |
| $c_p$ | = Specific heat | $\#/ft.^3$ |
| D | = Diameter | ft. |
| $D_e$ | = Equivelent diameter (excludes wall effects) | ft. |
| $D_{hy}$ | = Hydraulic Diameter (includes wall effects) | ft. |
| $D_R$ | = Heated rod diameter | ft. |
| $E_{g,\ell}$ | = Energy Generation terms for vapor, liquid | $BTU/ft.^3$-hr |
| F | = Chen coefficient | |
| $F_{g,\ell}$ | = $\alpha\rho_g, (1 - \alpha)\rho_\ell$ | $\#/ft.^3$ |
| $G_{g,\ell}$ | = $\alpha v_g \rho_g$, $(1 - \alpha)\ v_\ell \rho_\ell$ | $\#ft.^2$-hr |
| $G_o$ | = $G_g + G_e$ | |
| $h, h_g, h_\ell, h_{fg}, h_s$ | = Enthalpy; general, vapor, liquid, vaporization, saturation | BTU/# |
| $h_{g\ell}$ | = Evaporation enthalpy when liquid is not saturated | BTU/# |
| $h^*$ | = Film temperature enthalpy | BTU/# |
| $h_{A,B,C,D}$ | = Heat transfer coefficients: Hancox-Nicol, Thom, bulk condensation, Dittus-Boelter | $BTU/^oF\ ft.^2$-hr |
| $\bar{h}$ | = Heat transfer coefficient | |
| $h_m$ | = Microconvective coefficient | $BTU/^oF$-$ft.^2$-hr |
| $h_M$ | = Macroconvection coefficient | $BTU/^oF$-$ft.^2$-hr |
| $h_B^o$ | = Pressure dependent portion of the Thom relation | |

| | | |
|---|---|---|
| $k_{\ell,T}$ | = Thermal conductivity, liquid, turbulent | BTU/$^{o}$F-ft.-hr |
| J | = Conversion constant | |
| Ja | = Jacob number | |
| L ($\alpha$,p) | = Part of the slip correlation | |
| L | = Length of heated section | ft. |
| P | = Power generation rate in fuel (or heater)rod | |
| Pe | = Peclet number | |
| Pr | = Prandtl number | |
| p | = Pressure | #/ft.$^{2}$ |
| $p_{CR}$ | = Critical Pressure | |
| q" | = Surface heat generation rate | BTU/ft.$^{2}$hr |
| q"' | = Volumetric heat generation rate | BTU/ft.$^{3}$hr |
| $q"_{out}$ | = Surface heat generation rate leading to liquid phase heating | |
| Re | = Renolds number | |
| $Re_{\ell}$ | = Renolds number of liquid phase | |
| S | = Slip | |
| $S_t$ | = Stanton Number | |
| $S_{1,2}$ | = Indicators in the vapor generation rate term | |
| $t_c$ | = Condensation time of a bubble | |
| $t_{cps}$ | = Collapse time of a bubble | |
| $T_{\ell,g,w,s}$ | = Temperature of liquid, vapor, wall, saturation | $^{o}$F |
| T* | = Film temperature | |
| $T^*_{\ell}$ | = Temperature of subcooled liquid after bulk phase condensation | |
| V | = Volume | ft.$^{3}$ |
| $v_{g,\ell}$ | = Velocity of vapor,liquid | ft./hr |
| X | = Flow quality $\equiv G_g/G_o$ | |
| $X_{eq}$ | = Equilibrium quality $\equiv F_g/(G_g + F_\ell)$ | |
| $\alpha$ | = Void fraction | |
| $\beta$ | = $\rho_\ell(h_s - h_\ell)/(\rho_g h_{fg})$ | |

| | | |
|---|---|---|
| $(1 - \alpha)\eta P$ | = Energy directly deposited in the bulk | BUT/ft.$^3$-hr |
| $\rho_{g,\ell}$ | = Vapor, liquid densities | #/ft.$^3$ |
| $\dot{\Gamma}_g$ | = Vapor generation rate | |

## ABSTRACT

A mechanistic model for flow boiling in vertical geometries is developed and is qualified against steady-state void formation data. Extensive testing versus rod bundle data is included.

The model allows for subcooled void formation utilizing a modified Bancoff-Jones drift correlation. As established the model uses heat transfer and vapor generation correlations which are continuous at over the full range of parameters but does not utilize flow regime maps.

The correlations are qualified against tube, channel, and rod bundle voidage data. The qualification leads to excellent statistical agreement with the data:

| | | Void Fraction Mean Error | RMS Error | Number of Samples |
|---|---|---|---|---|
| Rod Bundles | = | -0.0002±0.0010 | 0.028 | 784 |
| Tubes | = | -0.0007±0.0010 | 0.022 | 440 |
| Channels | = | - .0021±0.0018 | 0.051 | 776 |

The purpose of this report is to establish and qualify (by comparison with data) a mechanistic model for predicting two-phase vertical flow in heated rod arrays and other vertical geometries. Particularly important for the use of the model in nuclear reactor analysis is its qualification against rod bundle data.

An earlier attempt at the establishment of such a model has been reported (1) and that model has been in use for some years. When the predictions of that model were recently examined statistically it was discovered that an approximately 5% negative bias ($\Delta \alpha/\alpha$) in rod bundle void fraction existed (Figure 1). With this as the impetus the earlier model and its constitutive relations were re-examined and new correlations have been established.

In qualifying the new model a much larger data base has been utilized consisting of a large number of additional rod bundle, rectangular channel and tube experiments along with the, mostly, channel experiments used in the first model's qualification. The present model has been optimized and the accuracy of the prediction can be seen in Figure 2.

The authors have found overall comparisons such as those presented in Figures 1 and 2 to be invaluable in determing model biases and trends. They are generally much more useful than comparisons with individual experiments.

This report consists of two parts and a number of appendicies.

PART 1: Model description

PART 2: Comparison with experimental data

APPENDIX A: Development of the vapor generation form

B: Choice of heat transfer coefficients

C: Slip modeling

D: Location of the Point of Net Vapor Generation

E: Liquid Phase Superheating

F: Comparisons with Individual Experiments

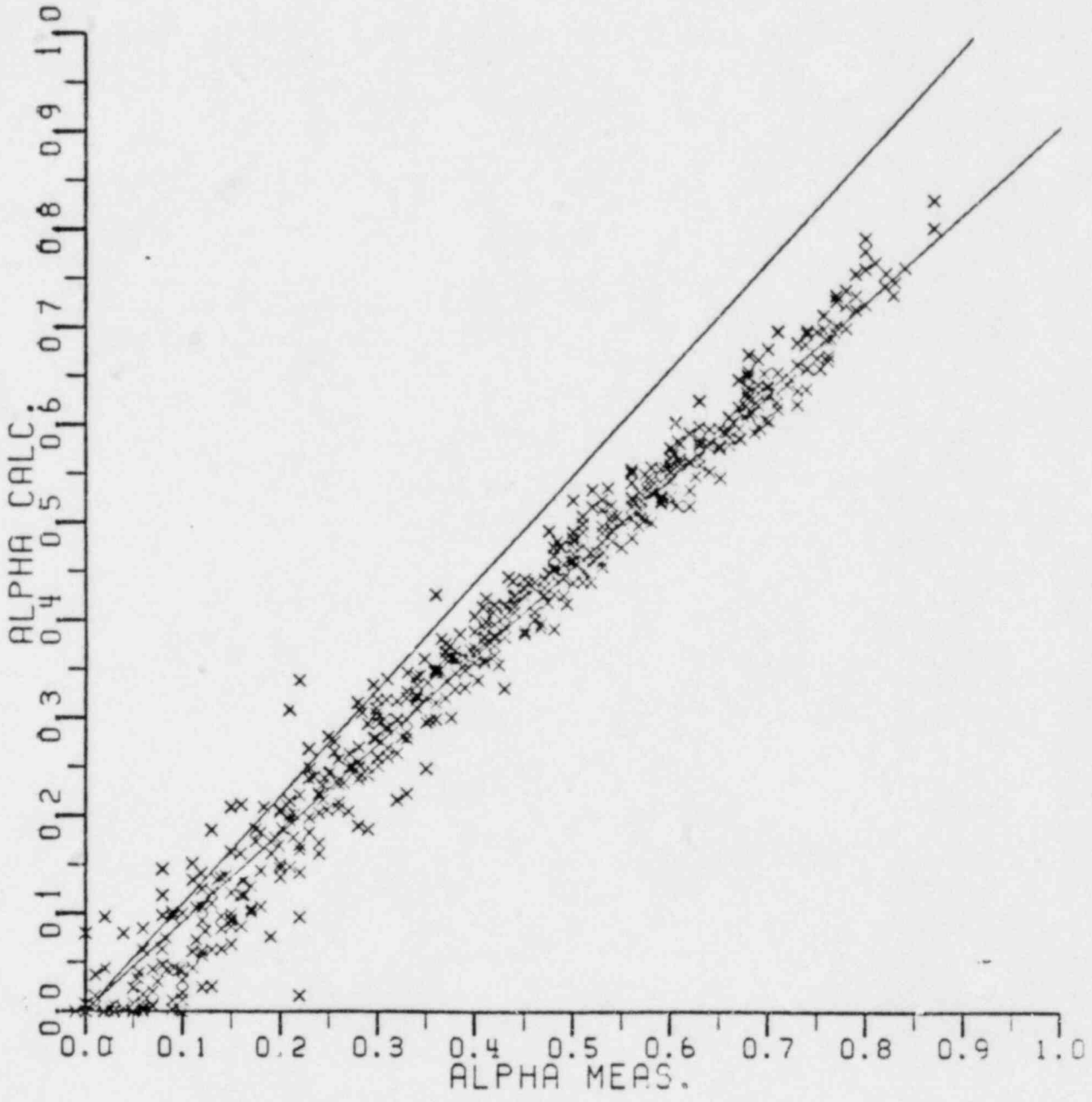


MODEL = 1

FRIGG DATA - LELLOUCHE/BNL MODEL

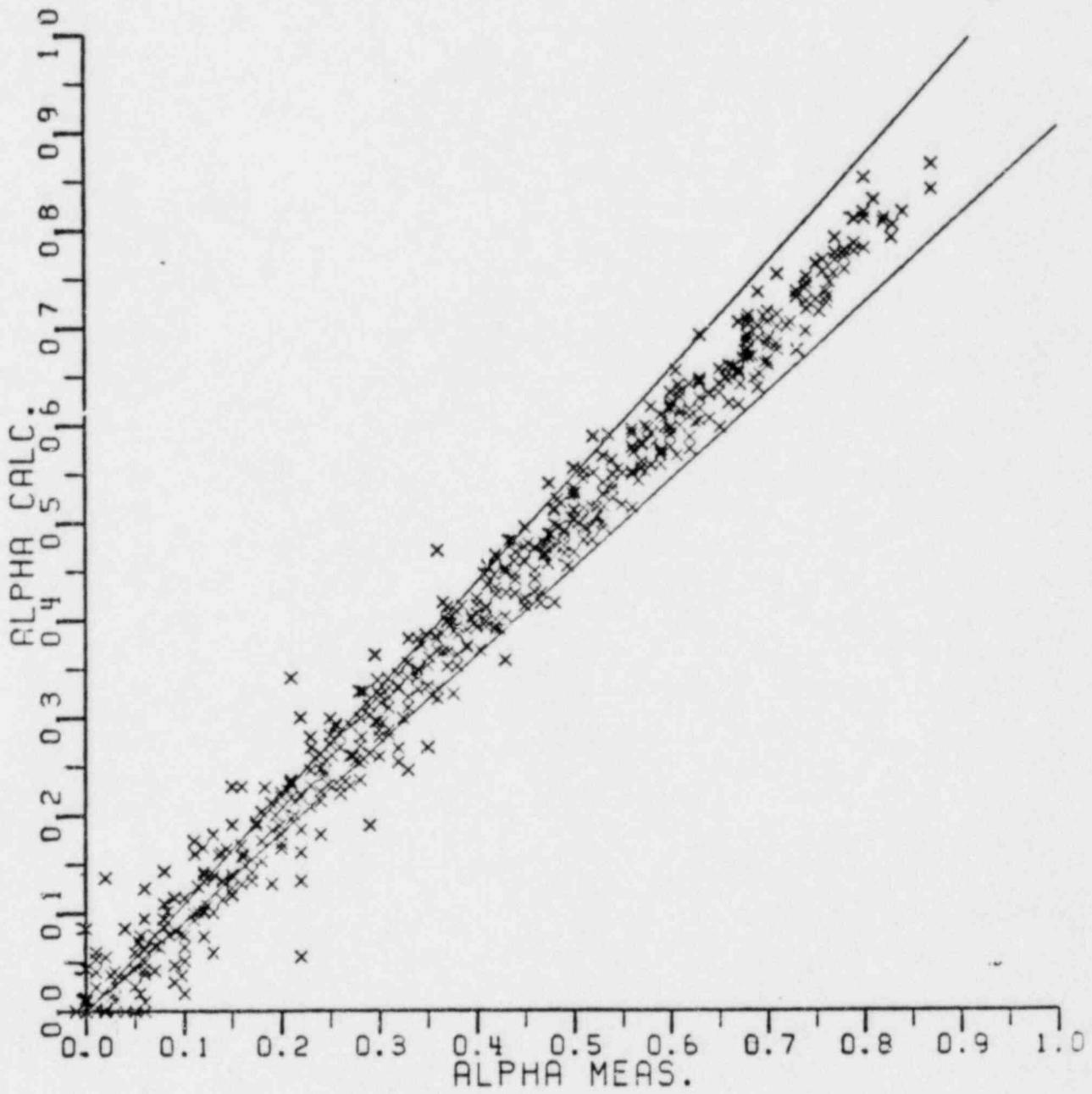


MODEL = 1

FRIGG DATA - REV CO AT LOW ALPHA

## PART 1: MODEL DESCRIPTION

### Conservation Equations

Basically we establish a four equation model: Two mass, one energy, and a quasi-momentum (drift-flux) relation.*

Mass conservation

$$\frac{\partial F_g}{\partial t} + \frac{\partial G_g}{\partial z} = \dot{\Gamma}_g \tag{1a}$$

$$\frac{\partial F_\ell}{\partial t} + \frac{\partial G_\ell}{\partial z} = -\dot{\Gamma}_g \tag{1b}$$

Energy conservation

We write the energy equation in enthalpy form

$$\frac{\partial (h_g F_g + h_\ell F_\ell)}{\partial t} + \frac{\partial (h_g G_g + h_\ell G_\ell)}{\partial z} = \frac{4}{D_e} q'' + q''' + \frac{1}{J}\frac{\partial p}{\partial t} \tag{2a}$$

In this form we neglect certain minor frictional components of the complete energy equation (see Ishii ). Here, the surface and volumetric heat sources are defined as (see ahead).

$$q'' = h_B (T_w - T_s) + h_D (T_w - T_\ell) \tag{2b}$$

and $$q''' = (1 - \alpha) n \quad P \tag{2c}$$

where P is the total energy developed in the heating element and n defines the direct deposition fraction (e.g. due to inelastic neutron scatter).

---

* The relationship between the momentum equations and the drift-flux model is derived in (_____).

The convection coefficients are taken as Dittus-Boelter ($h_D$) and Thom ($h_B$) coefficients.

Slip (quasi momentum balance)

Starting with a drift flux relation

$$v_g = C_o\,(\alpha v_g + (1 - \alpha)v_\ell) + v_{g\ell} \tag{3a}$$

we define the slip:

$$S \equiv \frac{v_g}{v_\ell} = \frac{1 - \alpha}{1 - C_o\alpha}\left[\; C_o + \rho_\ell v_{g\ell}/G_\ell \;\right] \tag{3b}$$

Constitutive Relations

The constitutive relations for the model are developed in a very general form and include effects and phenomena that are not qualified in this report but which will hopefully be qualified in the future. At the end of this section a description of the model actually qualified is presented.

I. Vapor Generation Relation

We consider the term $\dot{\Gamma}_g$ as being composed of three separate vapor sources:

- Vapor formed at the wall due to wall superheat
- Bulk boiling due to the direct deposition of energy (e.g. inelastic scatter of neutrons)
- Flashing and condensation due to transient pressure effects.

The derivation of the individual terms is discussed in Appendix A the final relation is taken as:

$$\dot{\Gamma}_g \equiv S_1 \left\{ \frac{q'' - q''_{out} - h_A(T_s - T_\ell)}{h_{fg}(1 + \beta)} \right\} \frac{4}{D_e} + S_2 \left\{ \frac{q''' - h_c\left(\frac{A}{V}\right)_c (T_s - T_\ell)}{h_{g\ell}} \right\}$$

$$- \frac{1}{h_{g\ell}} \left\{ \left( \frac{1}{J} \cdot F_g \frac{dh_g}{dp} + F_\ell \frac{dh_s}{dp} \right) \frac{\partial p}{\partial t} + \left( G_g \frac{dh_g}{dp} + G_\ell \frac{dh_s}{dp} \right) \frac{\partial p}{\partial z} \right\} \qquad (4a)$$

$$\beta \equiv \frac{\rho_\ell}{\rho_g} \frac{(h_s - h_\ell)}{h_{fg}} \qquad (4b)$$

The coefficients $S_{1,2}$ are zero until the bracketed terms become positive and then $S_{1,2} = 1$. If the bracket was positive and then becomes negative because of a change in power heat flux or power generation due to spatial or temperal effects the $S_{1,2}$ coefficient remains equal to 1 until all of the vapor has condensed.

II. Heat Transfer Relations

The heating process is made up of two parts

- Direct bulk heating and bulk condensation
- Surface heating and condensation

These processes are discussed in some detail in Appendix B; here we indicate only that the second follows from the following assumptions:

1. The wall heat flux ( $q''(z,t)$ ) is made up of micro-and macro-convective components. In a subcooled state micro-convection leads to vapor generation and macro-convection leads to heating of the liquid. At sauration both lead to vaporgeneration. Superheating of the liquid requires introduction of an evaporation coefficient (App. E).

2. The sum of these is taken as the sum of forced convection (i.e. Dittus-Boelter) and boiling (i.e. Thom) correlations.

3. Part of the forced convection heat transfer produces vapor when the film temperature is high enough hence is included in the micro-convection term.

4. The vapor generation term is proportional to the difference between the micro-convection heat transfer rate and a condensation term proportional to the bulk subcooling.

The first three conditions lead to the following:

$$q'' \equiv \underbrace{h_m (T_w - T_s)}_{\text{micro}} + \underbrace{h_M (T_w - T_\ell)}_{\text{macro}} \tag{5}$$

$$= (h_B + \tfrac{1}{2} h_D)(T_w - T_s) + \tfrac{1}{2} h_D (T_w - T_\ell + T_s - T_\ell) \tag{6}$$

Hence, we may define:

micro-convection: $(h_B + \tfrac{1}{2} h_D)(T_w - T_s)$

Macro-convection: $\tfrac{1}{2} h_D \left(1 + \dfrac{T_s - T_\ell}{T_w - T_\ell}\right)(T_w - T_\ell)$

The fourth condition states that:

$$\dot{\Gamma}_{gl} \propto (h_B + \tfrac{1}{2} h_D)(T_w - T_s) - h_A (T_s - T_\ell)$$

hence, (see eq (4) above) that:

$$q'' - q''_{out} = (h_B + \tfrac{1}{2}h_D)(T_W - T_\ell) \tag{7a}$$

$$q''_{out} = \tfrac{1}{2}h_D (T_W + T_S - 2T_\ell) \tag{7b}$$

The choice of heat transfer correlations, while key to the model development and application, selecting established forms and requiring as little adjustment of coefficients as possible. Here we have utilized:

Forced Convection

$$\text{Dittus-Boelter} \equiv h_D = C_D \; Re_\ell^{0.8} \; Pr_\ell^{0.4} \; k_\ell/D_{HY} \tag{8a}$$

and as developed by Weisman ( ) for rod bundles

$$C_D(\varepsilon) = 0.013 + 0.033\varepsilon \tag{8b}$$

$\varepsilon \equiv$ fraction of unit cell available for flow

This modeling of the coefficient, taken from the literature, appears valid for heating outside tubes. For heating other geometries we use the literature values appropriate to those geometries; e.g. 0.023 for rectangular geometries and tubes.

Boiling

$$\text{Thom} \equiv h_B = h_B^o \; (p)(T_W - T_S) \tag{9a}$$

$$h_B^o \; (p) = 193e^{\,p/630} \qquad \text{(English units)} \tag{9b}$$

Condensation near the Heater Surface

$$\text{Hancox-Nicol} \equiv h_A = C_A Re_\ell^{0.662} \; Pr_\ell k_\ell/D_R \tag{10a}$$

As is pointed out in the modeling of the vaporgeneration term (Appendix B) the original analysis leading to a value for $C_A$ (ie $C_A = 0.4$) was based on the assumption that all the surface heat flux went to vapor generation ($q''_{out} = 0$). In the present model this is not so, hence, the coefficient has been optimized against void data to give:

$$C_A = 0.2 \quad \text{for tubes and channels} \tag{10b}$$

$$= 0.1 \quad \text{for rod bundles} \tag{10c}$$

For rod bundles, the Nussult number in eq (10a) is based on the heated rod diameter (rather than the hydraulic diameter).

## III. The Distribution Coefficient

In eq (3) the distribution coefficient is introduced. We use a modification of the Bancoff-Jones coefficient.

$$\frac{1}{C_o} = (\kappa_1 + (1 - \kappa_1)\, \alpha^r) \,/L(\alpha) \tag{11}$$

where

$$\kappa_1 = \kappa_o + (1 - \kappa_o)\, (\rho_g/\rho_\ell)^{\frac{1}{2}} \tag{12a}$$

$$\frac{1}{\kappa_o} = 1 + e^{-Re/10^5} \tag{12b}$$

The relation for $\kappa_o$ depends on the inlet Renolds number. For tubes and rod bundles, data analysis (see Part II) indicates that $1/\kappa_0$ saturates at 1.25 (i.e., Re $>1.39 \times 10^5$).

The relation for r is found to be acceptably represented by

$$r = (1 + 1.57\ \rho_g/\rho_\ell) / (1 - \kappa_o) \tag{12c}$$

while the function L ($\alpha$) satisfies

$$L(\alpha) = (1 - e^{-C_1\alpha}) / (1 - e^{-C_1}) \tag{12d}$$

$$C_1 = 4\ p_{cr}^2 / (p\ (p_{cr} - p)) \tag{12e}$$

A detailed discussion of the slip model is found in Appendix C.

IV. The Drift Velocity

The term $v_{g\ell}$ in eq (3a) represents the gravitational effect on the vapor velocity. This term is most important at low liquid flow rates and is not trivially modeled. Nonetheless for the range of flows and pressures of interest at this time the term may be reasonably modeled as

$$v_{g\ell}(\alpha) = v^{o}_{g\ell}\ (1-\alpha)^{3/2} \tag{13a}$$

$$v_{g\ell}(o) = 1.41 \left[\frac{\rho\ell-\rho}{\rho_\ell^2}\ g g_c \sigma\right]^{1/4} \tag{13b}$$

V. The Qualified Model

Only two of the correlations discussed above are excluded from the qualification. They are the second and third parts of the vapor generation terms, eq (4a) (i.e., $\Gamma_{g_2}$ and $\Gamma_{g_3}$ of Appendix A). These terms have little impact on the type of data which was used in the qualification process. However, $\Gamma_{g_2}$, which describes direct energy deposition, is extremely important to BWR transient response in rod drop calculations. Thus, although a bulk condensation coefficient is not recommended here, it is recommended that $\Gamma_{g_2}$ be included utilizing the instantaneous condensation approximation in the subcooled regime and zero condensation in the post saturation regime.

Implicit also in the qualification is the fact that departure from nucleat bo ling is not accounted for. Thus, although the correlation $\Gamma_{g_1}$ produces accurate void fractions up into the 90% range no indication of whether DNB has occurred is produced by the model.

With these caveats the qua'ified model contains the follow correlations:

1. Vapor Generation

$$\Gamma_g = \Gamma_{g_1} \text{ (eq A4, c, d)} \tag{14}$$

2. Heat Tran,fer

a) Single Phase Subcooled

for $T_w<T_s$: $q'' = h_D (T_w-T_\ell)$ (15a)

for $T_w>T_{s\ell}$, and $T_w<T_D$

$$q'' = h_D(T_w-T_\ell) + h_B(T_w-T_s) \tag{15b}$$

$h_B$ from eq (3a, b)

at $T_w = T_D$

$T_D$ defined by

$$q'' = h_D (T_w - T_\ell) + h_B (T_D - T_s) \qquad (15c)$$

and $\Gamma_{g_1} = 0 \longleftrightarrow (h_B + \tfrac{1}{2} h_D)(T_D - T_s) = h_A (T_s - T_\ell)$ (15d)

$h_A$ from eq (10a-c)

b) Two-phase subcooled to saturated

$T_w > T_D$, $T_\ell \leq T_s$

$q''$ from eq (15b)

$\Gamma_g = \Gamma_{g_1} > 0$

$v_g$ from eq (3a)

$C_o$, $v_{g_\ell}$ from eq (11-13)

c) Two-phase superheated liquid

$q''$ from eq (15b)

$$\Gamma_{g_1} = 4 \left[ (h_D/2 + h_B)(T_w - T_s) + k_\ell N_u)E \ (T_\ell - T_s)/D_e \right] / h_{g_\ell} D_e \qquad (15e)$$

Nu)E from eq (E-8)

## PART 2: Comparison with Experimental Data

The development of the model and its later qualification involved the use of comparisons with extensive experimental void fraction data. All of the cases to be presented here are based on steady-state measurements in electrically heated test sections. Comparisons with transient data will be carried out in the future.

Experimental data were selected by the authors based on their applicability to water cooled nuclear reactors. The parameters of interest were flow rates, pressures, heat flux, inlet subcooling and geometry. However, a wide enough distribution of these parameters were selected so as to provide meaningful tests of the ability of the model to predict observed variations of void fractions under changed conditions. Some experiments were rejected based on the fact that their age cast doubt on their validity. Additionally, data at low pressures (less than 200 psi) and with other fluids than water were not utilized.

The rod bundle geometry data which have been utilized are characterized in Table 1. They are obviously the most important part of the comparisons. In addition to representing nuclear reactor conditions, they also appear to be of high quality. Figure 3 presents the comparison of all of this data with the model. Tables 2 and 3 show the statistical analysis which has been made. The model shows essentially a zero bias.

The degree of agreement is well demonstrated by examining each of the six sets of rod bundle data. Figures 4, 5, 6, 7, 8 and 9, together with Table 4 demonstrate that the results are essentially statistically equivalent. This is particularly significant because:

1. The FRIGG BWR experiments (although of only 36 rods) were very close to the geometry of current BWR designs. The geometries of the other sets of data were significantly different.
2. The FRIGG FT-36C experiments, with an axially dependent power distribution, were not utilized in determining the basic model "adjustment", hence tend to act as a "proof" of the model.
3. The CISE bundle experiments were carried out using a completely different technique (and at a different laboratory) than the FRIGG experiments.

The CISE and FRIGG data show about a 0.01 difference in void fraction between the measurement techniques. While more CISE data will be desirable to see if this is statistically significant, there is always a potential a a bias inherent in one or both techniques (e.g. there is a potential of a bias due to finite valve closing times in the CISE experiments).

TABLE 1

Rod Bundle Experiments

| | FRIGG FT-6 & 6A | FRIGG FT-36A | FRIGG FT-36B | FRIGG FT-36C | FRIGG 36 ROD BWR | CISE IT-25 |
|---|---|---|---|---|---|---|
| Number of heated rods | 6 | 36 | 36 | 36 | 36 | 19 |
| Type of rod array | Circular[1] | Circular[2] | Circular[2] | Circular[2] | Square[3] | Circular[4] |
| Rod diameter (ft) | .0456[5] | .0453 | .0453 | .0453 | Typical of 8x8 BWR Geometry | .0656 |
| Heated length (ft) | 14.50 | 14.35 | 14.32 | 14.32 | | 13.18 |
| Flow Area ($ft^2$) | .03298[6] | .1538 | .1538 | .1538 | | .0312 |
| Hydraulic diameter[7] (ft) | .1535[8] | .1201 | .1201 | .1201 | | .0318 |
| Axial heat distribution | Uniform | Uniform | Uniform | Non-uniform[9] | Uniform | Uniform |
| Radial heat distribution | Uniform | Uniform | Non-uniform[10] | Non-uniform[11] | Uniform | Non-uniform[12] |
| Measurement technique | γ-ray | γ-ray | γ-ray | γ-ray | γ-ray | Valves |
| Average pressure (psia) | 585 | 723 | 800 | 725 | 929 | 661 |
| Average flow rate $\left(\frac{MLB}{hr\text{-}ft^2}\right)$ | 0.980 | 0.798 | 0.789 | 0.705 | 1.105 | 1.366 |
| Average heat flux $\left(\frac{MBTU}{hr\text{-}ft^2}\right)$ | 0.167 | 0.123 | 0.157 | 0.191 | 0.154 | 0.128 |
| Reference | | | | | | |

TABLE 1 (cont.)

Rod Bundle Experiments (footnotes)

1. One central heated rod with five surrounding rods
2. One central unheated rod surrounded by three rings of rods containing 6, 12 and 18 rods respectively
3. A 6 by 6 square array of rods
4. A central heated rod surrounded by two rings of 6 and 12 rods respectively
5. 0.0453 feet for FRIGG FT-6A case
6. 0.03299 $ft^2$ for FRIGG FT-6A case
7. Hydraulic diameter defined as
   4 x (Flow Area in $ft^2$)/(Total Surface Area per foot)
8. 0.1545 feet for FRIGG FT-6A case
9. Peak to Average = 1.18
10. Peak to Average = 1.180
11. Peak to Average = 1.097
12. Peak to Average = 1.141

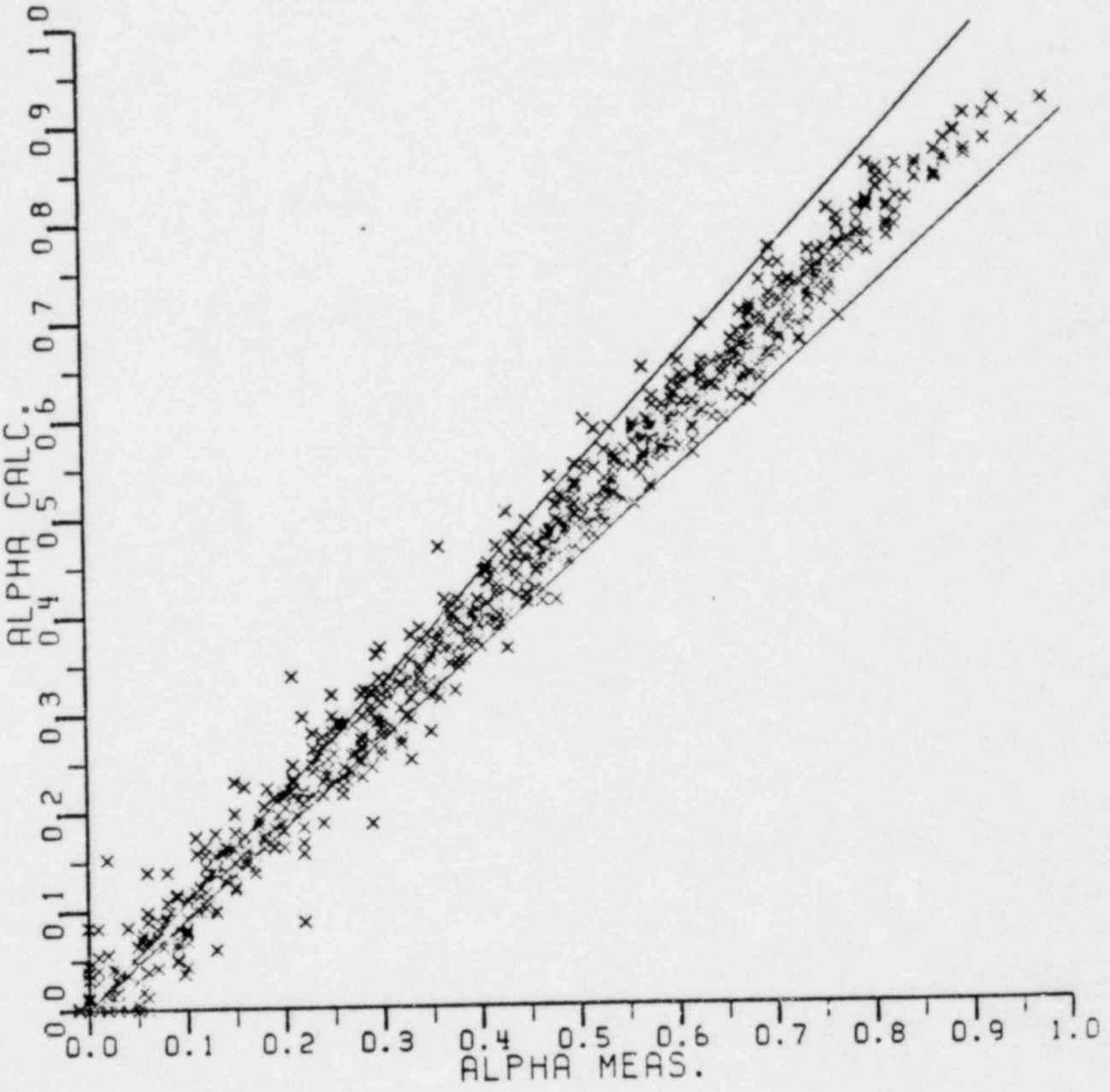


FIGURE 3: Model vs. All Rod Bundle Data

FIGURE 3 - Model vs All Rod Bundle Data

ATTACHMENT

$\alpha C$ =

$\alpha m$ =

$$\text{Average Error} = \epsilon = \sum_{n=1}^{n} \frac{(\alpha_c^n - \alpha_m^n)}{N}$$

$$\text{RMS Error} = \sigma = \sqrt{\sum_{n=1}^{N} \frac{(\alpha_c{}^n - \alpha_m{}^n - \epsilon)^2}{N-1}}$$

$$\text{Model Bias with Uncertainty} = \epsilon \pm \frac{\sigma}{\sqrt{N}}$$

N = Number of data points in sample

TABLE 2

Rod Bundles, Model vs Data
Statistical Analysis +

| $\alpha_m$ Range | Average Error $\varepsilon$ | RMS Error $\sigma$ | Sample Size N |
|---|---|---|---|
| $0.0 < \alpha_m \leq 0.1$ | -.0027 | .034 | 74 |
| $0.1 < \alpha_m \leq 0.2$ | .0043 | .028 | 67 |
| $0.2 < \alpha_m \leq 0.3$ | .0019 | .037 | 86 |
| $0.3 < \alpha_m \leq 0.4$ | -.0010 | .029 | 87 |
| $0.4 < \alpha_m \leq 0.5$ | .0027 | .026 | 110 |
| $0.5 < \alpha_m \leq 0.6$ | .0004 | .024 | 119 |
| $0.6 < \alpha_m \leq 0.7$ | -.0023 | .026 | 104 |
| $0.7 < \alpha_m \leq 0.8$ | -.0041 | .024 | 81 |
| $0.8 < \alpha_m \leq 0.9$ | -.0060 | .022 | 30 |
| $0.9 < \alpha_m \leq 1.0$ | -.0336 | .022 | 5 |
| All $\alpha_m$* | .0002 | .028 | 784 |

Model Bias = -.0002 ± .0010

+Attachment
*includes $\alpha_m \leq 0.0$ values

TABLE 3

Rod Bundles, Model vs Data
Error Distribution

| $\alpha_c - \alpha_m$ | Fraction in Range |
|---|---|
| < -0.15 | 0.000 |
| -0.15 to -.10 | 0.003 |
| -0.10 to -0.05 | 0.031 |
| -0.05 to 0.00 | 0.488 |
| 0.00 to 0.05 | 0.440 |
| 0.05 to 0.10 | 0.034 |
| 0.10 to 0.15 | 0.004 |
| > 0.15 | 0.000 |

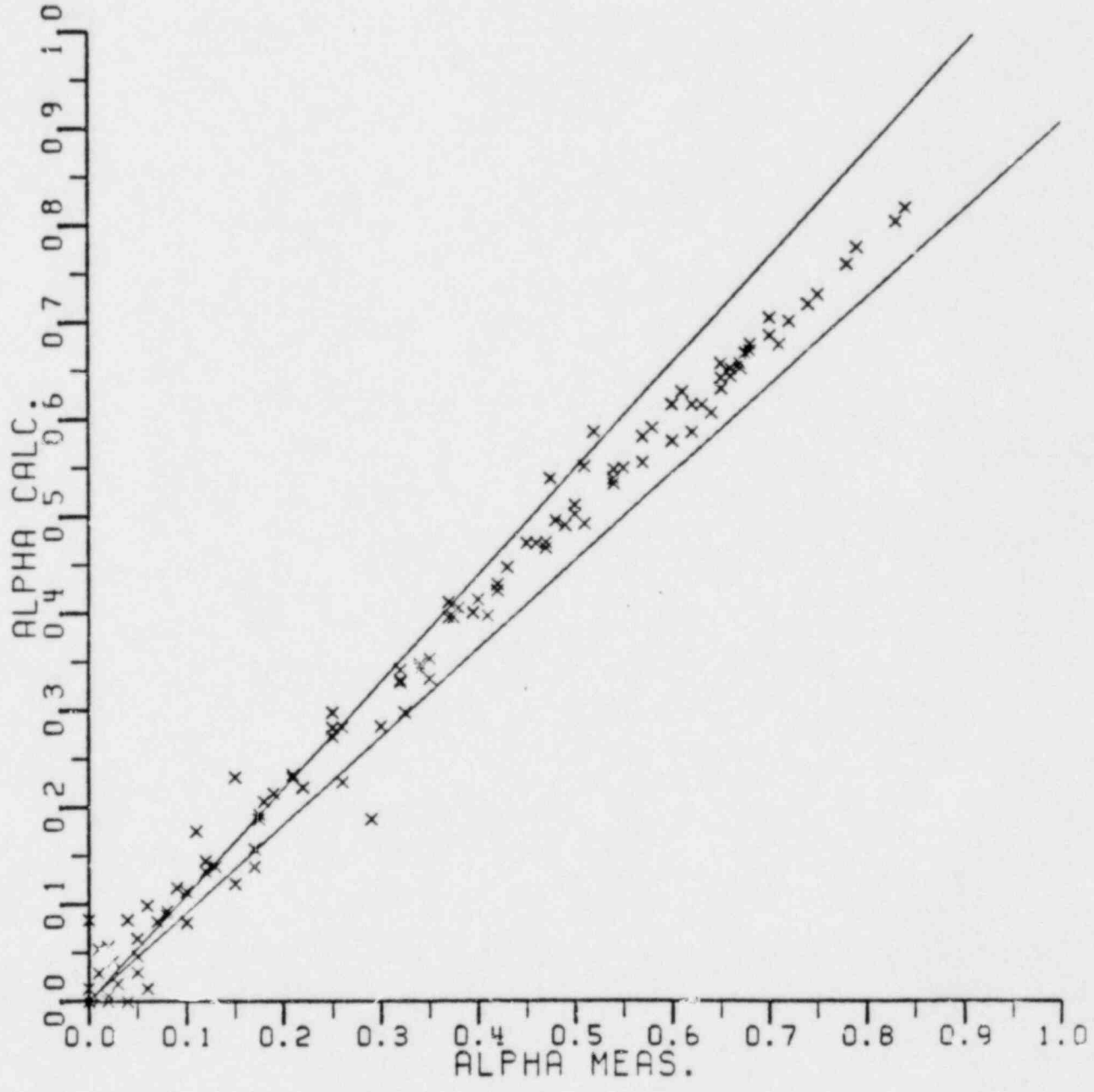


FIGURE 4 - Model vs.

FRIGG FT-6 & FT-6A DATA

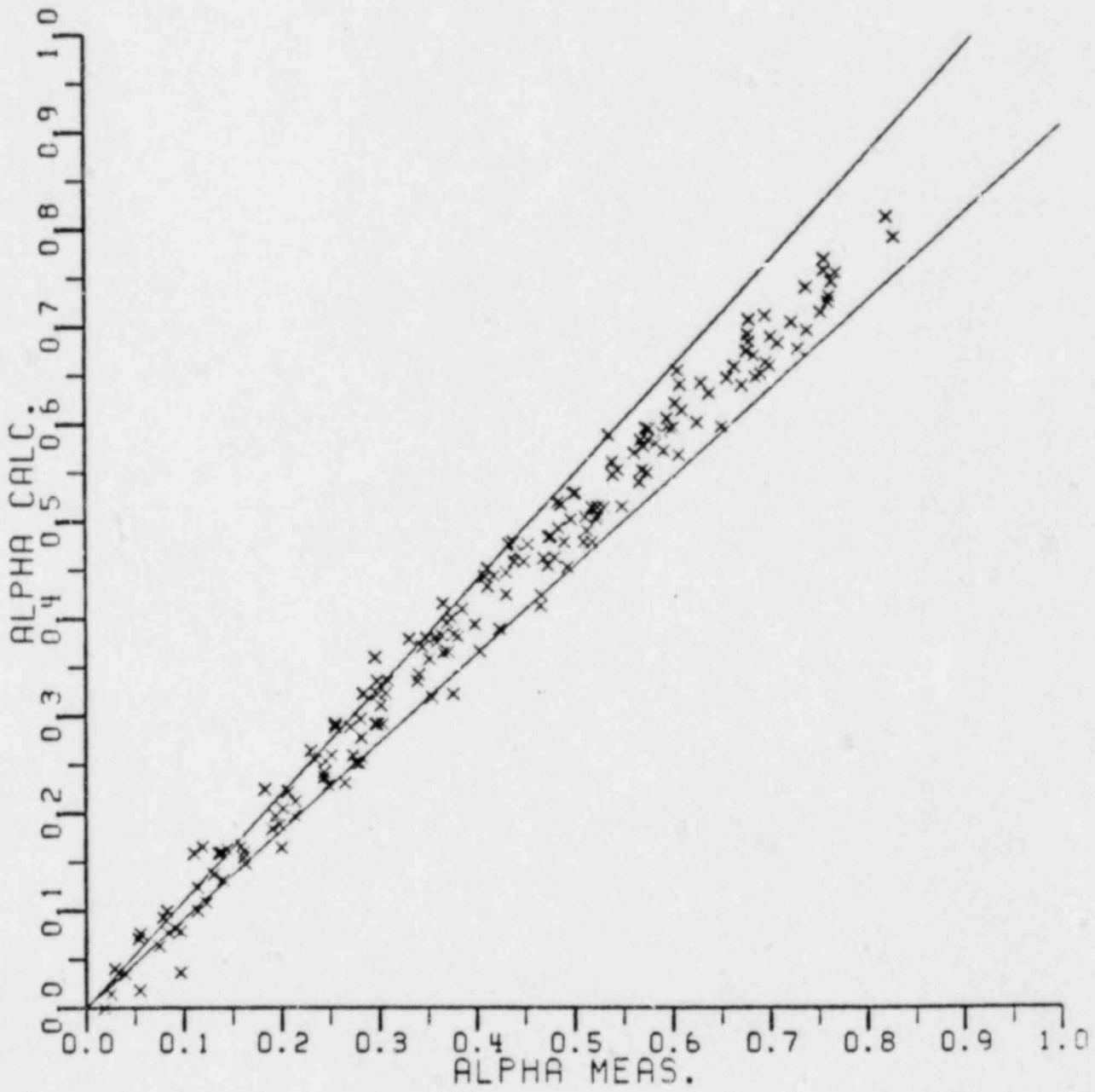


FIGURE 5 - Model vs.

FRIGG FT-36A DATA

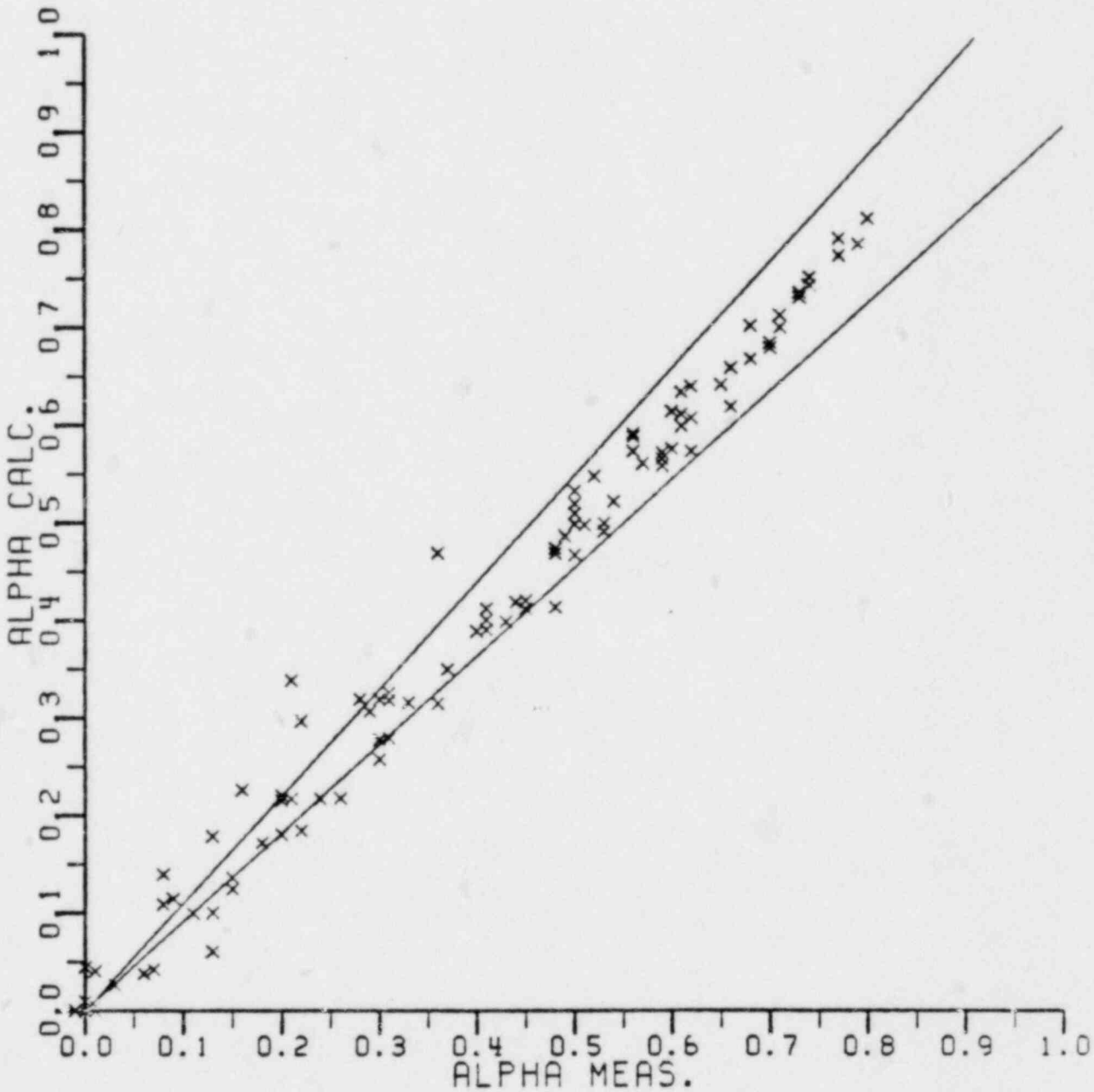


FIGURE 6 - Model vs.

FRIGG FT-36B DATA

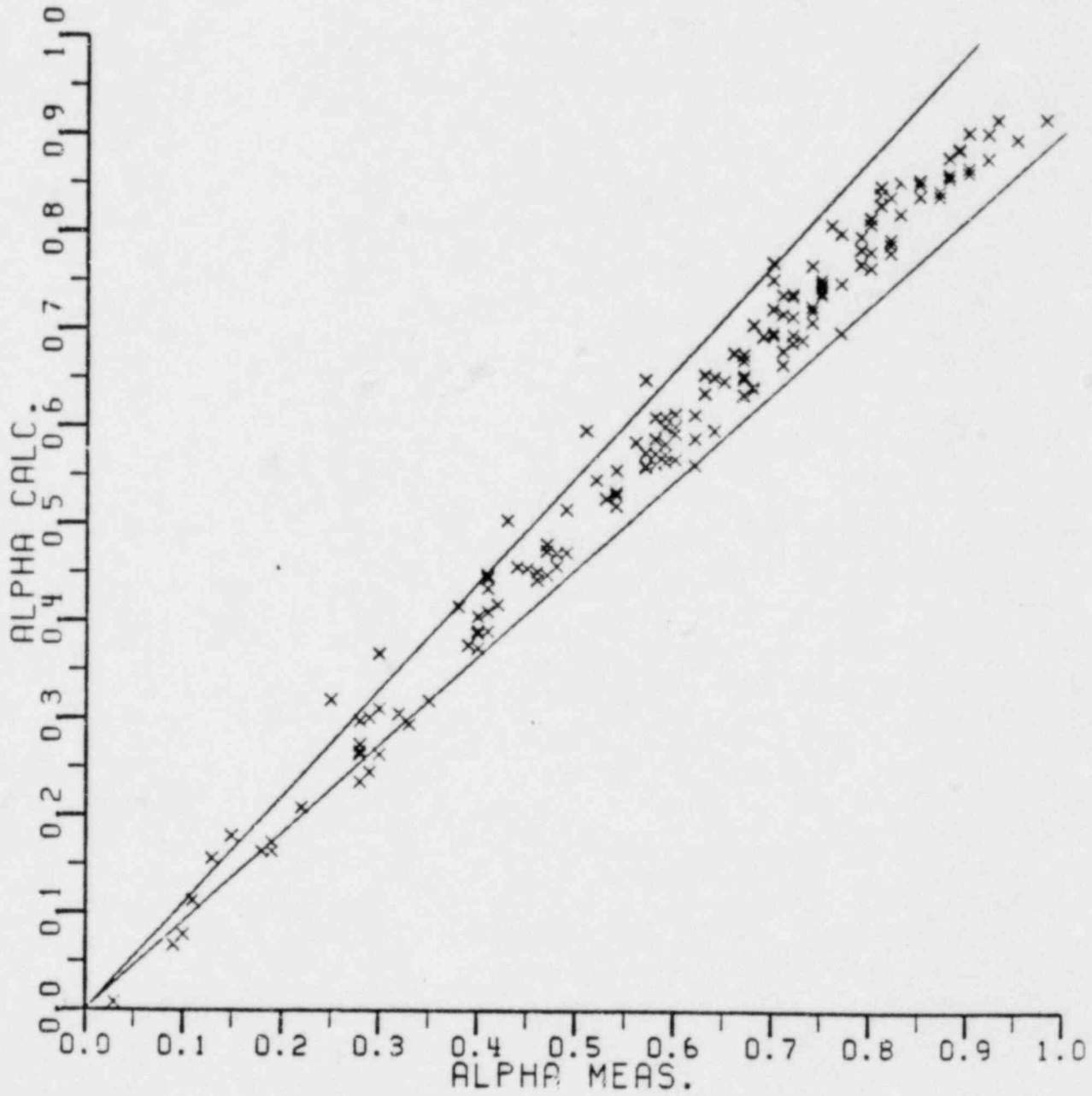


FIGURE 7 - Model vs.

FRIGG FT-36C DATA

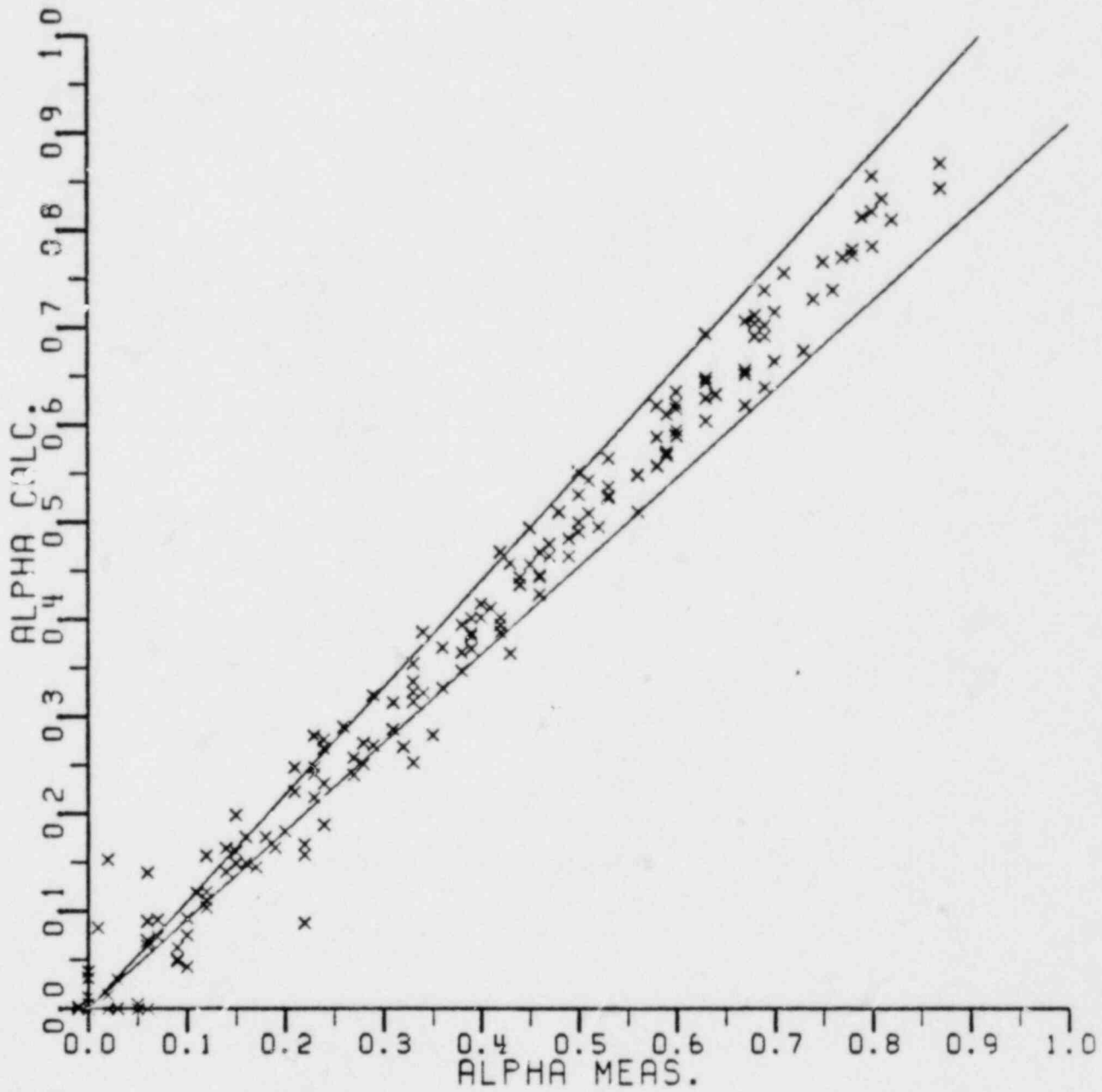


FIGURE 8 - Model vs.

FRIGG 36 ROD BWR DATA

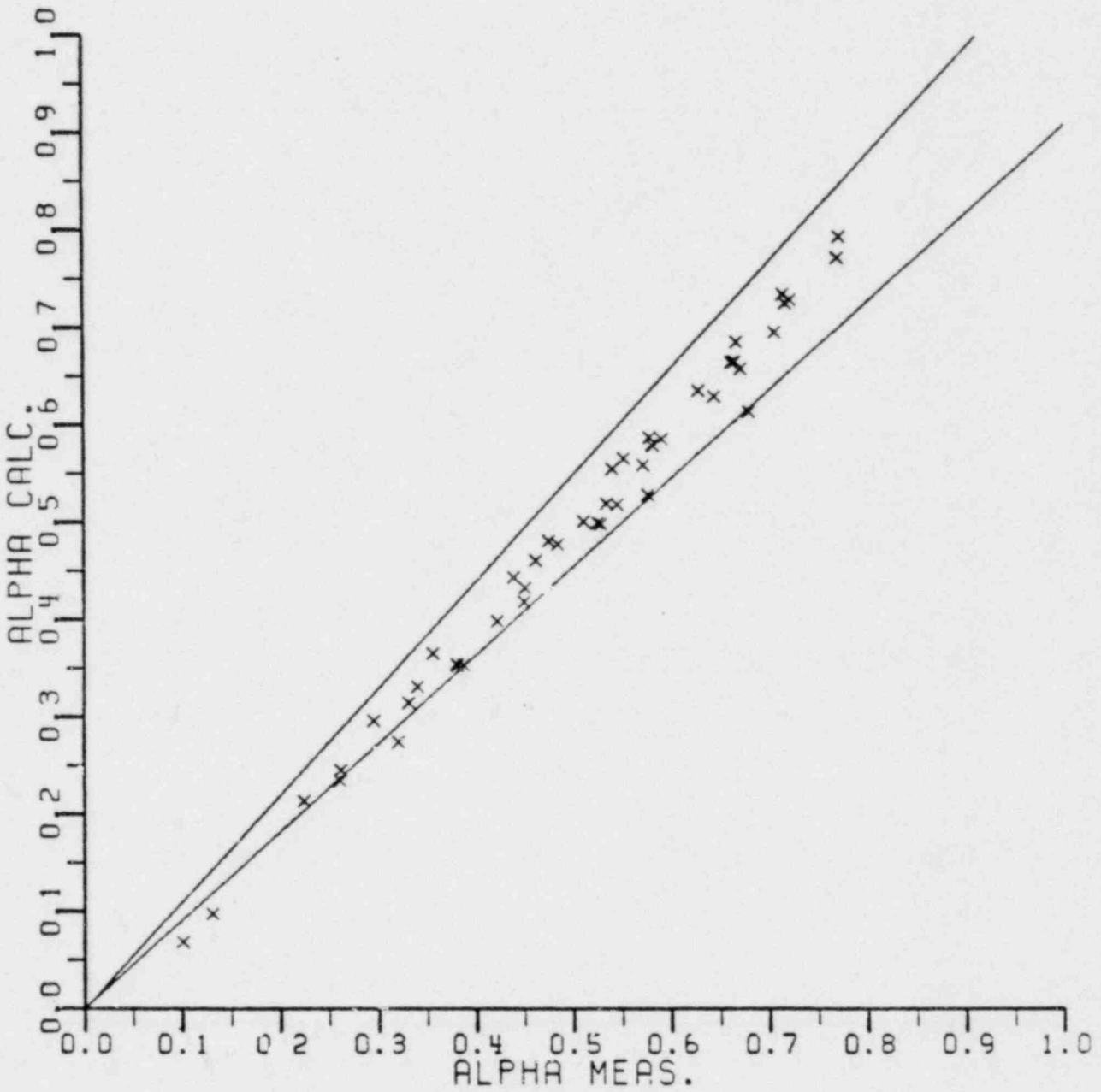


FIGURE 9 - Model vs.

CISE ROD BUNDLE DATA

TABLE 4

Rod Bundles, Model vs Data
Analysis of Experimental Sets

| Set | Model Bias | RMS Error σ | Sample Size N |
|---|---|---|---|
| FRIGG FT-6 & FT-6A | .0047±.0024 | .026 | 118 |
| FRIGG FT-36A | .0014±.0019 | .025 | 180 |
| FRIGG FT-36B | .0002±.0031 | .031 | 101 |
| FRIGG FT-36C | -.0013±.0022 | .028 | 157 |
| FRIGG 36 Rod BWR | -.0017±.0024 | .032 | 182 |
| All FRIGG Data | .0004±.0011 | .029 | 738 |
| CISE Bundle Data | -.0098±.0029 | .019 | 46 |
| All Bundle Data | -.0002±.0010 | .028 | 784 |

TABLE 5

Rectangular Channel Experiments

| | Maurer | St. Pierre | Christensen | Martin |
|---|---|---|---|---|
| Heated length (ft) | 2.250 | 4.200 | 4.167 | 3.310-4.950 |
| Flow area ($ft^2$) | .0006-.0007 | .0053 | .0053 | .0011-.0016 |
| Hydraulic diameter[1] (ft) | .0133-.0147 | .0583 | .0583 | .0131-.0184 |
| Axial heat distribution | Uniform | Uniform | Uniform | Uniform |
| Measurement technique | γ-ray | γ-ray | γ-ray | γ-ray |
| Average pressure (psia) | 1493 | 456 | 629 | 1598 |
| Average flow rate $\left(\frac{MLB}{hr\text{-}ft^2}\right)$ | 0.958 | 0.598 | 0.618 | 1.136 |
| Average heat flux $\left(\frac{MBTU}{hr\text{-}ft^2}\right)$ | 0.405 | 0.056 | 0.113 | 0.259 |
| Reference | | | | |

1. Defined as in Table 1, footnote #7

TABLE 6

Round Tube Experiments

| | IT-23 | RT |
|---|---|---|
| Heated length (ft) | 3.281-13.451 | 6.562 |
| Tube diameter (ft) | 0.0301 | 0.0295 |
| Axial Heat distribution | Uniform | Uniform |
| Measurement technique | Valve | Valve |
| Average pressure (psia) | 650 | 589 |
| Average flow rate $\left(\frac{MLB}{hr\text{-}ft^2}\right)$ | 1.023 | 1.166 |
| Average heat flux $\left(\frac{MBTU}{hr\text{-}ft^2}\right)$ | 0.242 | 0.236 |
| Reference | | |

In order to extend the range of conditions available for testing the model, comparisons have also been made to a number of void fraction measurements from heated rectangular channels and round tubes. Tables 5 and 6 show the characteristics of these experiments. Figure 10 and Tables 7 and 8 again show the statistical analysis which has been made on the channel data. Figures 11, 12, 13 and 14, and Table 9 provide the comparisons for each of the different experimentors. It can be seen that there is some inconsistency between the measurements made by the various experimentors. In particular, the Martin data appears to be about 4% higher than the other data. This may be due to differences in experimental techniques. However, because of its relatively low statistical scatter and wide pressure range, the Martin data was particularly useful in formulating the pressure variation for the slip relationship. Figure 15 and Tables 10 and 11 show the statistical analysis for the CISE tube data. This data was important in formulating the flow dependence in Co.

It is also important to show that the model can follow the observed trends in void fraction with conditions. Table 12 shows the predictions of the model in different ranges of pressure and flow. The influence of these quantities appears to be reasonably well described by the model.

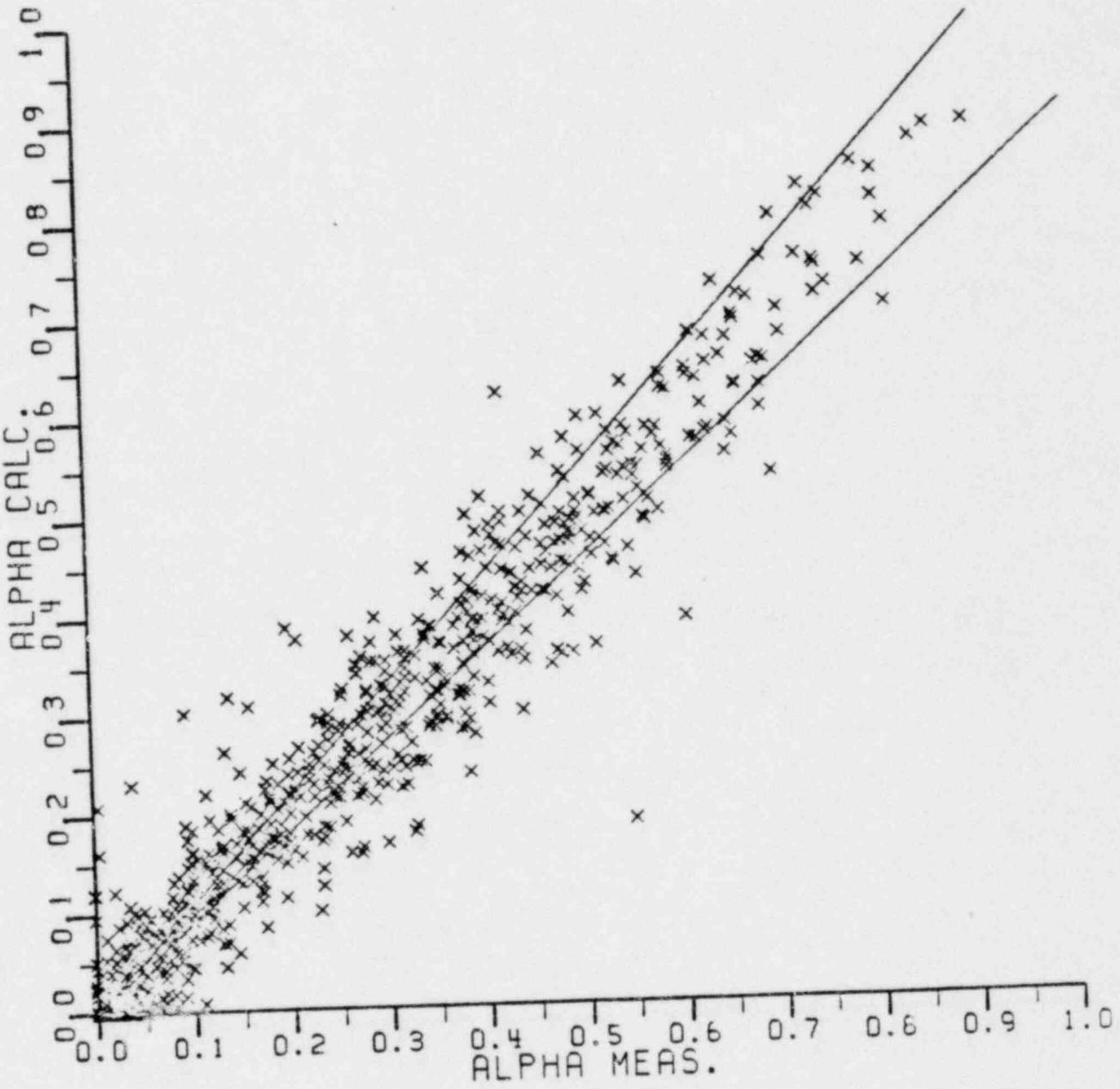


FIGURE 10 - Model vs.
All rectangular
CHANNEL DATA

TABLE 7

Rectangular Channels, Model vs Data
Statistical Analysis

| $\alpha_m$ Range | Average Error $\varepsilon$ | RMS Error $\sigma$ | Sample Size N |
|---|---|---|---|
| $0.0 < \alpha_m \leq 0.1$ | .0028 | .037 | 257 |
| $0.1 < \alpha_m \leq 0.2$ | .0067 | .050 | 105 |
| $0.2 < \alpha_m \leq 0.3$ | -.0003 | .054 | 102 |
| $0.3 < \alpha_m \leq 0.4$ | -.0158 | .057 | 96 |
| $0.4 < \alpha_m \leq 0.5$ | -.0070 | .061 | 76 |
| $0.5 < \alpha_m \leq 0.6$ | -.0245 | .069 | 50 |
| $0.6 < \alpha_m \leq 0.7$ | -.0141 | .069 | 32 |
| $0.7 < \alpha_m \leq 0.8$ | .0181 | .047 | 12 |
| $0.8 < \alpha_m \leq 0.9$ | -.0052 | .050 | 7 |
| $0.9 < \alpha_m \leq 1.0$ | --- | --- | 0 |
| All $\alpha_m$* | -.0021 | .051 | 776 |

Model Bias = -.0021 ± .0018

*includes $\alpha_m \leq 0.0$ values

TABLE 8

Rectangular Channels, Model vs Data
Error Distribution

| $\alpha_c - \alpha_m$ | Fraction in Range |
|---|---|
| < -0.25 | 0.001 |
| -0.25 to -0.20 | 0.001 |
| -0.20 to -0.15 | 0.001 |
| -0.15 to -0.10 | 0.025 |
| -0.10 to -0.05 | 0.114 |
| -0.05 to 0.00 | 0.420 |
| 0.00 to 0.05 | 0.309 |
| 0.05 to 0.10 | 0.102 |
| 0.10 to 0.15 | 0.016 |
| 0.15 to 0.20 | 0.007 |
| 0.20 to 0.25 | 0.004 |
| > 0.25 | 0.000 |

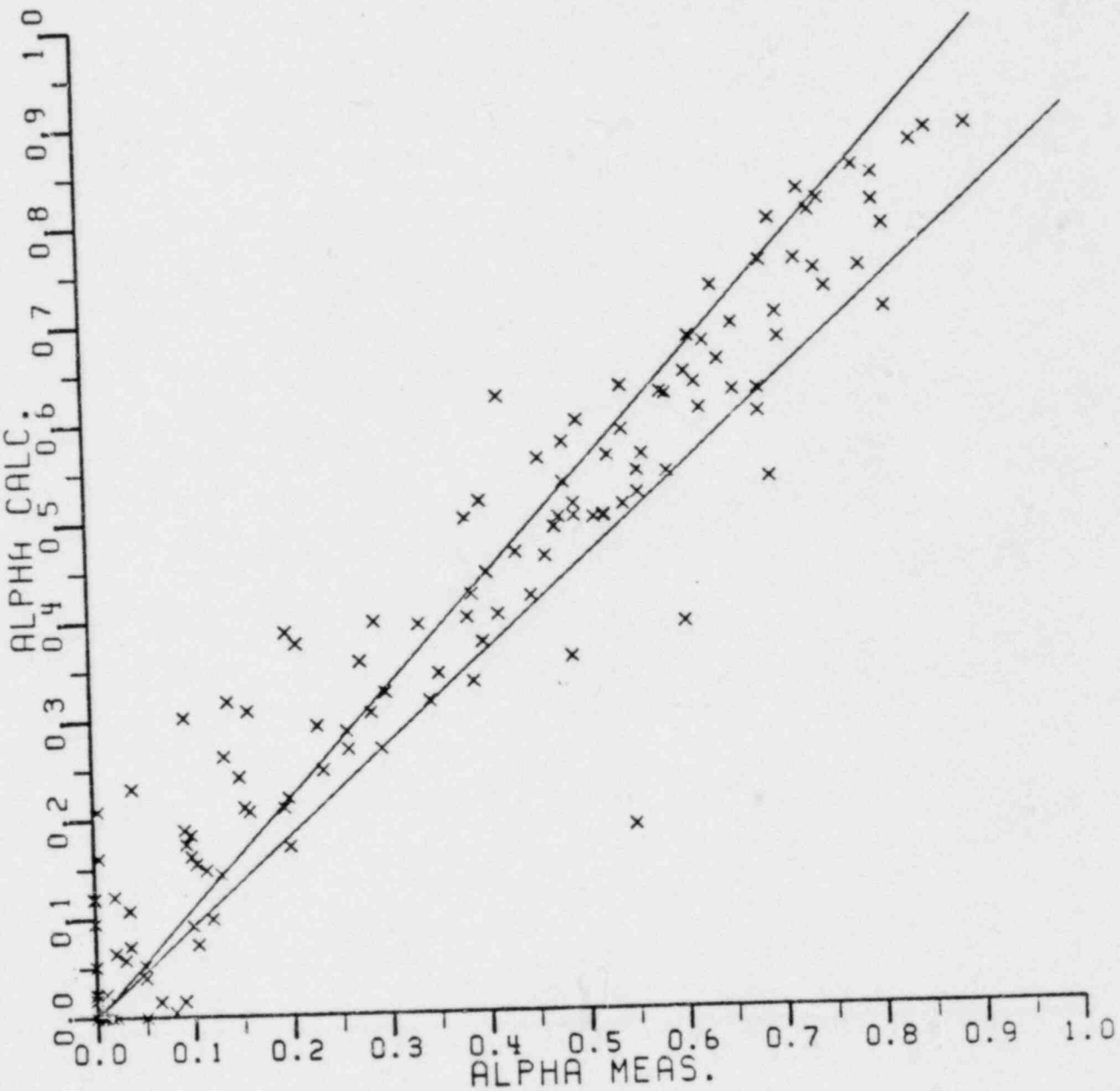


FIGURE 11 - Model vs.

MAURER CHANNEL DATA

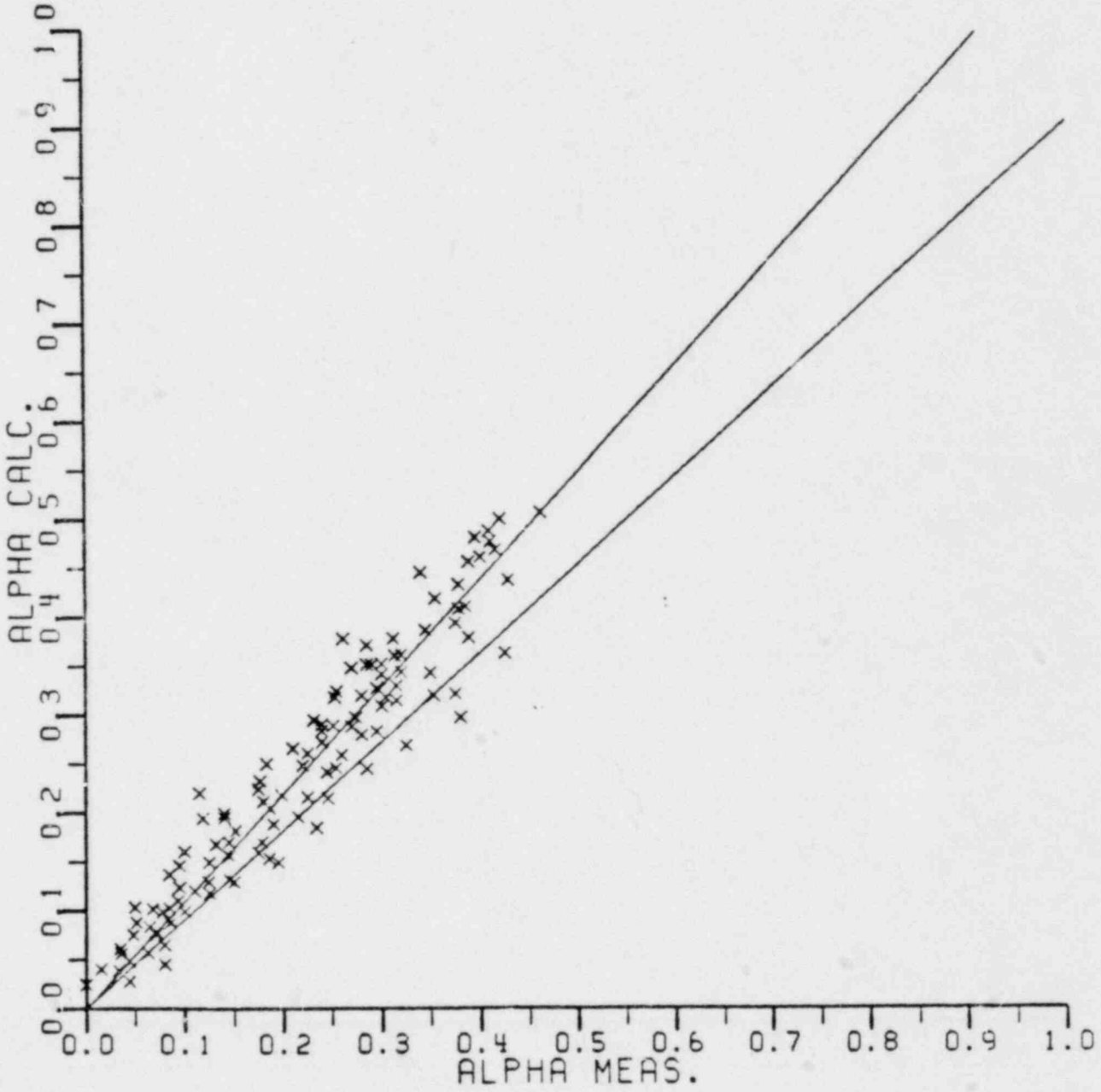


FIGURE 12 - Model vs.

ST. PIERRE CHANNEL DATA

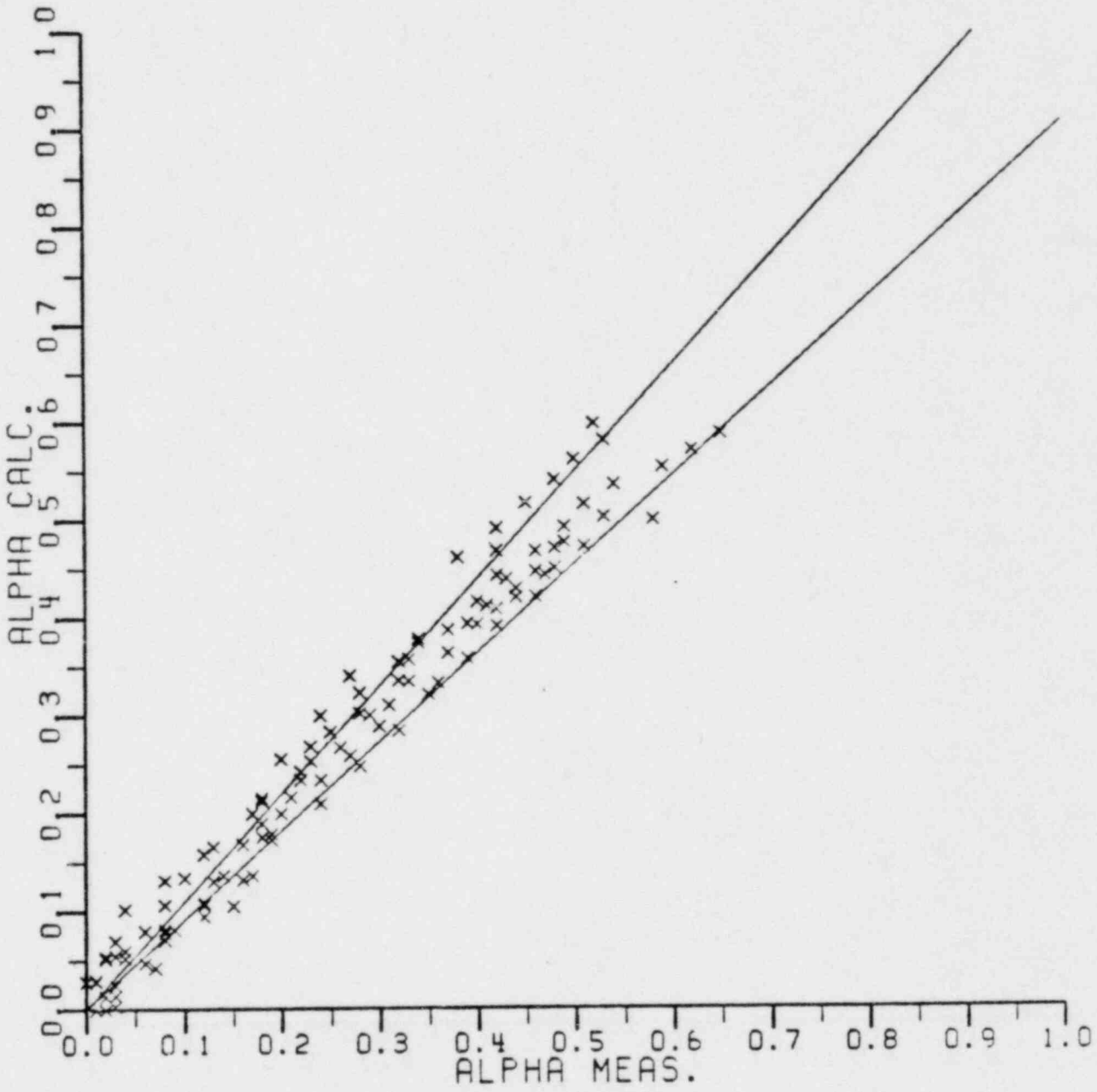


FIGURE 13 - Model vs.

CHRISTENSEN CHANNEL DATA

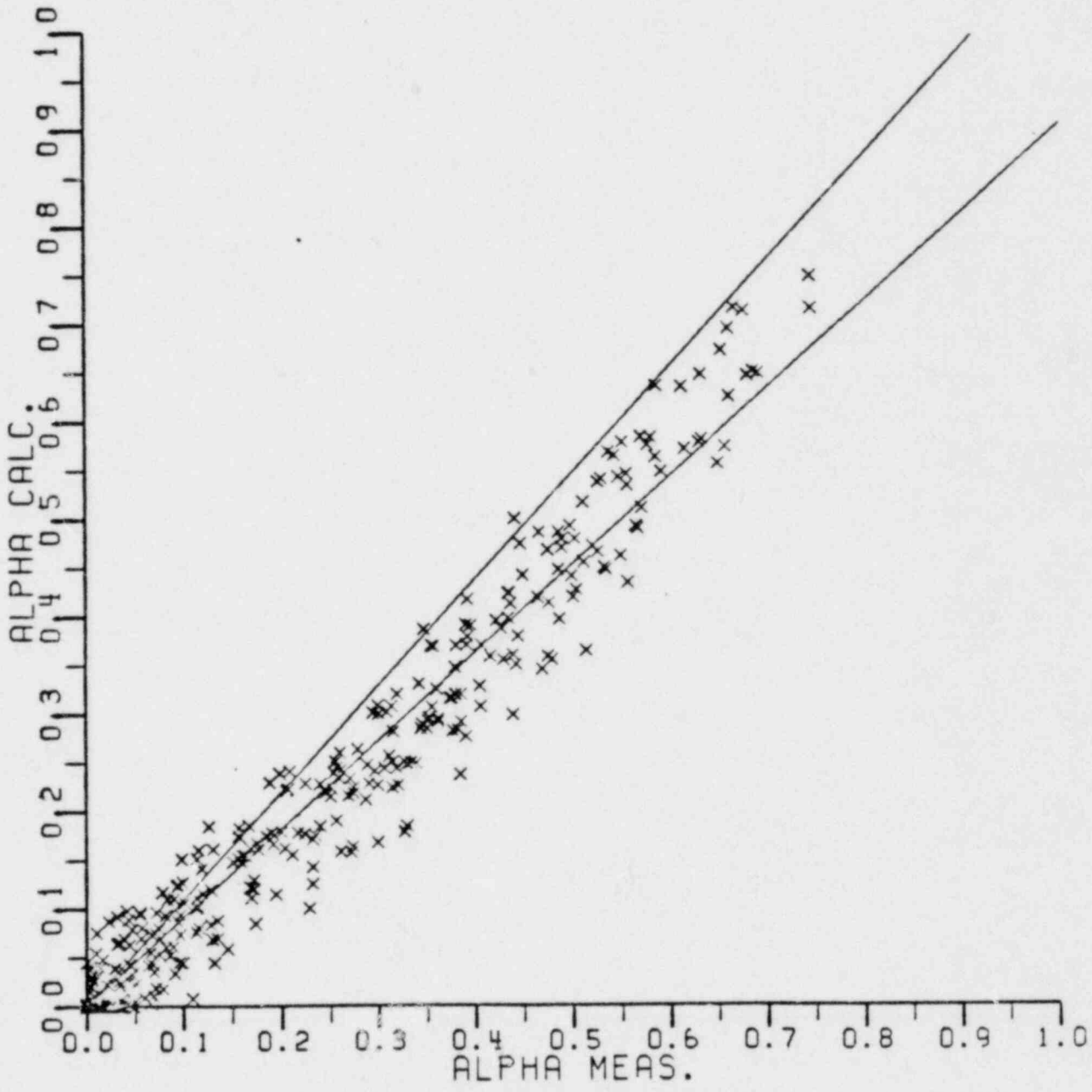


FIGURE 14 - Model vs.

MARTIN CHANNEL DATA

TABLE 9

Rectangular Channels, Model vs Data
Analysis of Experimental Sets

| Set | Model Bias | RMS Error σ | Sample Size N |
|---|---|---|---|
| Maurer | .0253±.0068 | .077 | 133 |
| St. Pierre | .0249±.0035 | .038 | 115 |
| Christensen | .0070±.0030 | .032 | 112 |
| Martin | -.0208±.0019 | .039 | 416 |
| All Channel Data | -.0021±.0018 | .051 | 776 |

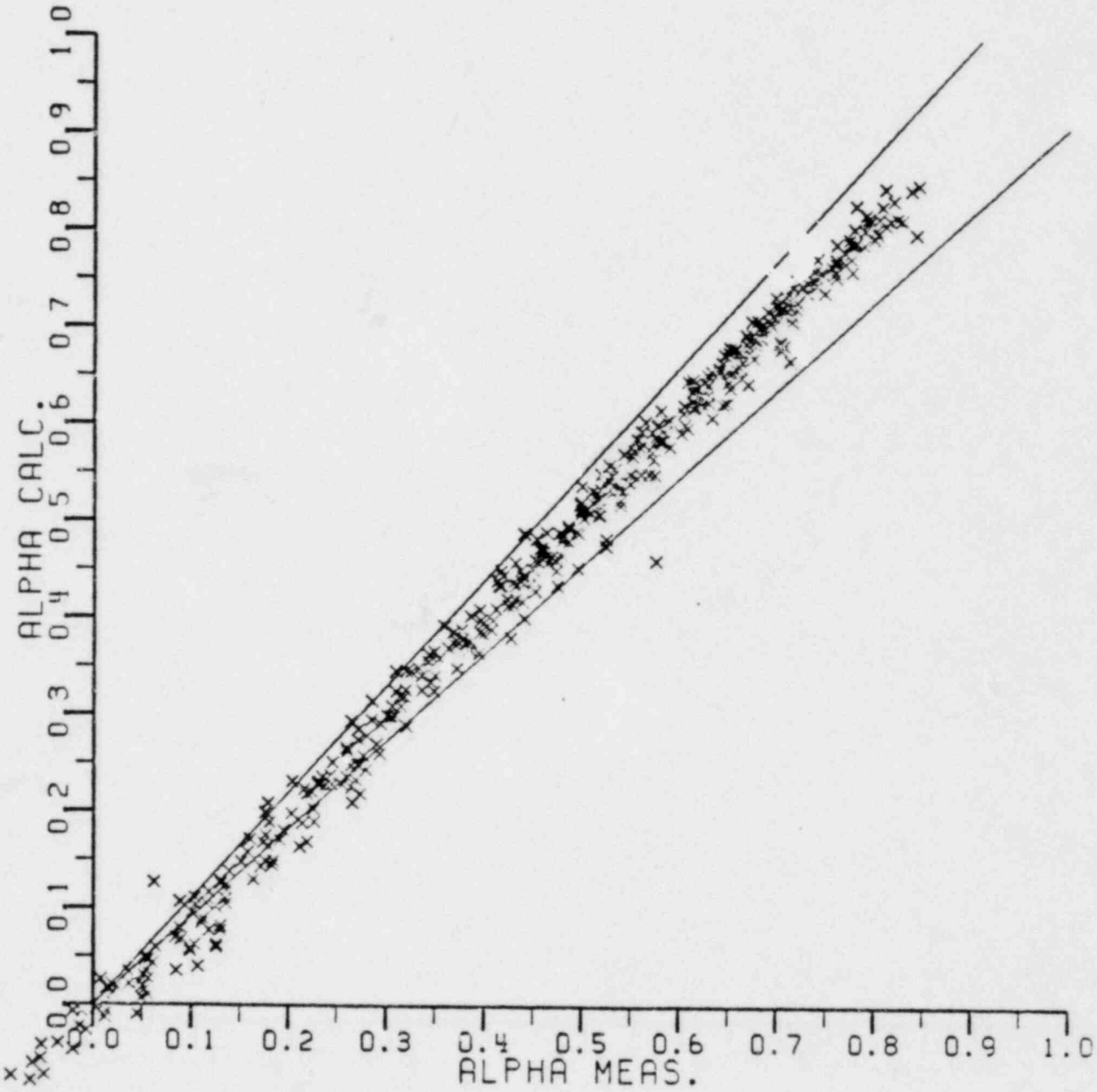


FIGURE 15 - Model vs.

CISE TUBE DATA

TABLE 10

CISE Tube Data, Model vs Data
Statistical Analysis

| $\alpha_m$ Range | Average Error $\varepsilon$ | RMS Error $\sigma$ | Sample Size N |
|---|---|---|---|
| $0.0 < \alpha_m \leq 0.1$ | -.0153 | .023 | 33 |
| $0.1 < \alpha_m \leq 0.2$ | -.0187 | .023 | 38 |
| $0.2 < \alpha_m \leq 0.3$ | -.0120 | .022 | 41 |
| $0.3 < \alpha_m \leq 0.4$ | .0022 | .015 | 43 |
| $0.4 < \alpha_m \leq 0.5$ | .0026 | .019 | 60 |
| $0.5 < \alpha_m \leq 0.6$ | .0050 | .023 | 63 |
| $0.6 < \alpha_m \leq 0.7$ | .0116 | .014 | 77 |
| $0.7 < \alpha_m \leq 0.8$ | .0100 | .016 | 60 |
| $0.8 < \alpha_m \leq 0.9$ | .0014 | .019 | 13 |
| $0.9 < \alpha_m \leq 1.0$ | --- | --- | 0 |
| All $\alpha_m$* | -.0007 | .022 | 440 |

Model Bias = -.0007 ± .0010

* includes $\alpha_m \leq 0.0$ values

TABLE 11

CISE Tube Data, Model vs Data
Error Distribution

| $\alpha_c - \alpha_m$ | Fraction in Range |
|---|---|
| < -0.15 | 0 |
| -0.15 to -0.10 | .002 |
| -0.10 to -0.05 | .016 |
| -0.05 to 0.00 | .400 |
| 0.00 to 0.05 | .580 |
| 0.05 to 0.10 | .002 |
| >0.10 | 0 |

TABLE 12

Model vs Data

Pressure and Flow Range Comparisons

| Configuration | All Data | | Pressure Ranges in PSI | | | | | | | | Flow Range in MLB/HR- $FT^2$ | | | |
|---|---|---|---|---|---|---|---|---|---|---|---|---|---|---|
| | | | $P \leq 700$ | | $700 \leq P \leq 1000$ | | $1000 \leq P \leq 1500$ | | $P \geq 1500$ | | $1.0 \leq G$ | | $G \geq 1.0$ | |
| | Bias ±σ | Sample Size | Bias ±σ | Sample Size | Bias ±σ | Sample Size | Bias ±σ | Sample Size | Bias ±σ | Sample Size | Bias ±σ | Sample Size | Bias ±σ | Sample Size |
| Rod Bundles | -.0002 ±.0010 | 784 | .0027 ±.0023 | 189 | .0000 ±.0012 | 479 | -.0051 ±.0025 | 140 | --- | 0 | .0010 ±.0012 | 546 | -.0030 ±.0018 | 238 |
| Channels | .0021 ±.0018 | 776 | .0192 ±.0027 | 184 | .0026 ±.0047 | 43 | -.0137 ±.0044 | 187 | -.0072 ±.0026 | 378 | -.0011 ±.0024 | 510 | -.0042 ±.0028 | 266 |
| Tubes | -.0007 ±.0010 | 440 | .0032 ±.0022 | 128 | -.0003 ±.0011 | 312 | --- | 0 | --- | 0 | -.0007 ±.0013 | 281 | .0033 ±.0016 | 159 |

Appendix A

## Establishing the Vapor Generation Term

As stated in the body of the paper, the term $\dot{r}_g$ is considered as being composed of three separate vapor sources:

- Vapor formed at the wall due to wall superheat
- Bulk boiling due to the direct deposition of energy (e.g. inelastic scatter of neutrons)
- Flashing and condensation due to transient pressure effects.

1. Vapor generated at the wall.

In deriving a model for this term we assume the existance of a superheated boundry layer (B.L.) of liquid at the wall with an average temperature:

$$T^* = (T_w - T_s)/2 > T_s \qquad (A1)$$

That is, at the film temperature. We account for the process (assumed to be in dynamic equilibrium) of creation of voids, displacement of mass into and out of the B.L. and bulk, and due to condensation just outside the B.L. Mixing is assumed to occur faster than the time scales of interest. The edge of the B.L. is assumed to be where $T_\ell = T_s$, but its location and the actual volume of the B.L. does not concern us. The characterization of the B.L. and the rest of the channel is made through $T^*$ and $T_\ell$, except that liquid leaving the B.L. is assumed to be at $T_s$.

Consider the following sketch:

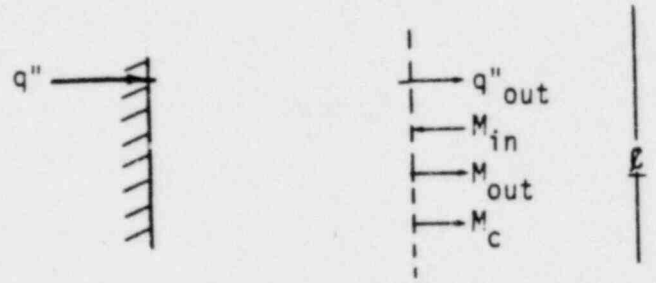


$q'' = h_D(T_w - T_\ell) + h_B(T_w - T_s)$ : Boiling + Non boiling Terms (See App. B)

$q'' - q''_{out}$ = boiling potential in the B.L. (See App. B)

$M_{in}$: = Measures the mass of liquid returning to the B.L. from the bulk liquid due to a bubble leaving the B.L.

$M_{out}$: measures the mass of gas leaving the B.L. and entering the bulk liquid

$M_c$: measures the mass of liquid leaving the B.L. and entering the bulk due to condensation of bubbles at the B.L. (this is assumed to occur on the same time scale as other mass interchanges).

Balancing over the region we find:

Mass: $M_{in} = M_{out} + M_c$

Energy: $q'' + \overline{M_{in}\, h}_{in} = q''_{out} + \overline{M_{out}\, h}_{out} + \overline{M_c h_c}$

If $V_g$ is the rate of bubble formation, $V_\ell$ the rate of liquid mass return, and $V_c$ the rate of liquid mass leaving the B.L. due to condensation in the bulk then: *

$\alpha \rho_g V_g$ = vapor mass leaving the B.L.

$\alpha(\rho_\ell - \rho_g)V_g$ = excess mass of liquid leaving B.L. due to creation of the voids in the B.L.

$\alpha(\rho_\ell - \rho_g)\, V_c$ = mass of liquid leaving B.L. due to condensation at the B.L.

Clearly, the net rate of vapor formation is given by:

$$\alpha\rho_g\,(V_g - V_c) = \dot{\Gamma}_{gl} \tag{A2}$$

If all energy terms are measured from the local bulk liquid temperature (or enthalpy) we find;

$$\overline{M_{out}h_{out}} = \left[\alpha\rho_g(h_g - h_\ell) + \alpha(\rho_\ell - \rho_g)\,(h_s - h_\ell)\right] \quad Vg$$

$$\overline{M_{in}h_{in}} = \alpha\rho_\ell V_\ell\,(h_\ell - h_\ell) = 0$$

$$\overline{M_c h_c} = \alpha\,(\rho_\ell - \rho_g)\,(h_s - h_\ell)\,V_c$$

The energy term $\alpha\rho_g\,(h_g - h_\ell)\,V_c$ due to condensation in the bulk is not counted since it is contained in the equivalent $V_g$ term.* There are 3 unknowns ($V_g$, $V_\ell$, $V_c$) and only two equations. We assume the existance of a heat transfer correlation, unspecified as yet, which accounts for near surface condensation and set

$$\alpha\rho_g\,V_c\left[h_g - h_\ell + \frac{(\rho_\ell - \rho_g)}{\rho_g}(h_s - h_\ell)\right] = \bar{h}\,(T_s - T_\ell) \tag{A3}$$

*The vapor is assumed to be formed at the saturation temperature rather than the film temperature. Except for massive transients this should have little impact.

The estimation of $\bar{h}$ (see A4d) is discussed in Appendix B. From eq (10) we find progressively

$$\alpha\rho_g V_g h_{fg} (1 + \beta) = q'' - q''_{out} - \alpha\rho_g h_{fg}\beta V_c \tag{A4a}$$

$$\beta = \frac{\rho_\ell}{\rho_g} \frac{(h_s - h_\ell)}{h_{fg}} \tag{A4b}$$

$$\dot{\Gamma}_{gl} \equiv \alpha\rho_g (V_v - V_\ell) = S_1 \left\{ \frac{q'' - q''_{out} - (1 + 2\beta)\bar{h}(T_s - T_\ell)/(1+\beta)}{h_{fg}(1+\beta)} \right\} \frac{4}{D_e} \tag{A4c}$$

$S_1$ = o in the subcooled regime only up to the point where the bracket becomes >0, thereafter $S_1$ = 1.

Finally, set

$$h_A = (1 + 2\beta)\bar{h} / (1 + \beta) \tag{A4d}$$

The term $q_{out}$ is defined in the standard way through the film temperature

$$q''_{out} = h_D (T^* - T_\ell) \tag{A5}$$

hence

$$\Delta q'' \equiv q'' - q''_{out} = h_D (T_v - T^*) + h_B (T_w - T_s) = (h_B + \tfrac{1}{2}h_D)(T_w - T_s) \tag{A6}$$

This completed the derivation of $\dot{\Gamma}_{gl}$ (the surface heat term).

2. Vapor Generated due to direct energy deposition

Since we do not account for superheating of the vapor due to direct

deposition we have a vapor mass increase rate

$$\alpha\rho_g V_g^D = q'''/h_{g\ell} = (1 - \alpha)\, nP/h_{g\ell}$$

$$h_{g\ell} \equiv h_g - h_\ell$$

and the rate of bulk condensation (with condensation heat transfer coefficient $h_c$)*

$$\alpha\rho_g V_g^{DC} = h_c\left(\frac{A}{V}\right)_c (T_s - T_\ell)/h_{g\ell}$$

The net rate of formation is then given by

$$\Gamma_{g2} \equiv \alpha\rho_g (V_g^D - V_g^{DC})$$
$$= S_2 \left\{ \frac{(1-\alpha)\, n\, P - h_c \left(\frac{A}{V}\right)_c (T_s - T_\ell)}{h_{g\ell}} \right\} \qquad \text{(A7)}$$

and $S_2 = 0$ if the bracket term is negative, otherwise $S_2 = 1$.

The determination of the term $h_c(A/V)_c$ will be discussed in Appendix B.

3. Vapor Generation due to transient and spatial pressure effects

Consider an expansion of the energy equation (eq 2A) leading to

$$h_g \left(\frac{\partial F_g}{\partial t} + \frac{\partial G_g}{\partial z}\right) + h_s \left(\frac{\partial F_\ell}{\partial t} + \frac{\partial G_\ell}{\partial z}\right) + F_g \frac{\partial h_g}{\partial t} + G_g \frac{\partial h_g}{\partial z} + F_\ell \frac{\partial h_s}{\partial t} + G_\ell \frac{\partial h_s}{\partial z}$$

$$+ \frac{\partial (h_\ell - h_s) F_\ell}{\partial t} + \frac{\partial (h_\ell - h_s) G_\ell}{\partial z} = \frac{4}{D_e} q'' + q''' + \frac{1}{J} \frac{\partial p}{\partial t} \qquad \text{(A8)}$$

* Note that the condensation term proposed by Hancox and Nicol is a surface condensation effect characterized by the surface area of the heat source. For the bulk effect we must somehow deal with the surface area of the voids. This is discussed in App. B.

where we have added and subtracted the term:

$$\frac{\partial h_s F_\ell}{\partial t} + \frac{\partial h_s G_\ell}{\partial z} \quad .$$

Using eq (1a,b) we can rewrite this as

$$h_{fg}\,\dot{\Gamma}_g + F_g \frac{\partial h_g}{\partial t} + G_g \frac{\partial h_g}{\partial z} + F_\ell \frac{\partial h_s}{\partial t} + G_\ell \frac{\partial h_s}{\partial z} + \frac{\partial (h_\ell - h_s) F_\ell}{\partial t} + \frac{\partial (h_\ell - h_s) G_\ell}{\partial z}$$

$$= \text{R.H.S.} \qquad \text{(A9)}$$

If we assume that $h_g$ and $h_s$ are only pressure dependent (equalibrium thermal-dynamics) then the derivatives in the second to fifth terms on the left side of eq (A9) are only pressure dependent and can be replaced by terms like:

$$\frac{dh_g}{dp} \frac{\partial p}{\partial t} \quad ; \quad \frac{dh_s}{dp} \frac{\partial p}{\partial z} \quad .$$

When $h_\ell \rightarrow h_s$ the last two terms on the right side go to zero (neglecting superheat of the liquid for the moment); hence, the direct pressure effect of $\dot{\Gamma}_g$ must be

$$\dot{\Gamma}_{g3} = -\frac{1}{h_{g\ell}} \left\{ \left( -\frac{1}{J} + F_g \frac{hg}{dp} + F_\ell \frac{dhs}{dp} \right) \frac{\partial p}{dt} + \left( G_g \frac{dh_g}{dp} + G_\ell \frac{dh_s}{dp} \right) \frac{\partial p}{\partial z} \right\} \qquad \text{(A10)}$$

and the full vapor generation term is

$$\dot{\Gamma}_g = \dot{\Gamma}_{g1} + \dot{\Gamma}_{g2} = \dot{\Gamma}_{g3}$$

$$= S_1 \left\{ \frac{(q'' - q''_{out} - h_A (T_s - T_\ell) \frac{4}{De}}{h_{fg} (1 + B)} \right\} + S_2 \left\{ \frac{q''' - h_c \left(\frac{A}{V}\right)_c (T_s - T_\ell)}{h_{g\ell}} \right\}$$

$$- \frac{1}{h_{g\ell}} \left\{ \left( -\frac{1}{J} + F_g \frac{dh_g}{dp} + F_\ell \frac{dh_s}{dp} \right) \frac{\partial p}{\partial t} + \left( G_g \frac{dh_g}{dp} + G_\ell \frac{dh_s}{dp} \right) \frac{\partial p}{\partial z} \right\} \qquad \text{(A11)}$$

It should be emphasized that $\dot{\Gamma}_g$ is a mass splitting relation. The energy equation (eq 2a) can however be split given the form of $\dot{\Gamma}_g$ . Suppose

$$\frac{\partial h_g F_g}{\partial t} + \frac{\partial G_g h_g}{\partial z} = E_g$$

$$\frac{\partial h_\ell F_\ell}{\partial t} + \frac{\partial G_\ell h_\ell}{\partial z} = E_\ell$$

$$E_\ell + E_g = \frac{4}{D_e} q'' + q''' + \frac{1}{J} \frac{\partial p}{\partial t}$$

Then using eq (1a) and eq (A11) we have

$$E_g = h_g (\dot{\Gamma}_{g1} + \dot{\Gamma}_{g2}) - \left( \left( \frac{1}{J} + F_\ell \frac{\partial h_s}{dp} \right) \frac{\partial p}{\partial t} + G_\ell \frac{dh_s}{dp} \frac{\partial p}{\partial z} \right)$$

and $E_\ell$ follows directly.

Equation (A9) defines $\Gamma_g$ hence in the saturated regime, neglecting pressure effects for the moment, we must have

$$h_{fg} \dot{\Gamma}_g = \frac{4}{D_e} q'' + q'''.$$

Equation (A11) however states (setting $S_{1,2} = 1$)

$$h_{fg} \dot{\Gamma}_g = \frac{4}{D_e} (q'' - q''_{out}) + q'''$$

hence, $q''_{out}$ must $\to 0$ as $T_\ell \to T_s$. The definition of $q''_{out}$ (eq (7b) and eq (A5) shows however that

$$q''_{cut} \to \frac{1}{2} h_D (T_w - T_s) \neq 0$$

This fact implies either that the liquid superheats ($T_\ell > T_s$) or that we change the model setting $q''_{out} \equiv 0$ (accounting for pressure effects does not alter this conclusion). In fact we believe that the liquid phase does superheat and this aspect of the model is discussed in App. E.

## Appendix B

### Choice of Heat Transfer Coefficients

It has been the view of the authors that the "adjusting" of the model should be minimized. We have, within the structures of the postulated phenomenalogical basis of the model, chosen heat transfer coefficients from the literature. Only one such coefficient has been "adjusted" and the rationale for that is described below.

The phenomena that are assumed to underly the processes of heating and ultimately vaporizing the liquid are:

- o forced convection heat transfer wall to boundry layer (B.L.) to bulk
- o Void formation in the film
- o Subcooled condensation just outside the B.L.
- o Direct heating of the liquid phase
- o Bulk condensation

The model as established does not consider the variation of heat transfer coefficient with flow regime and no use of flow maps is allowed. he logic of the model allows various heating modes, however, which are discussed below.

1. Forced Convection Heat Transfer

When the surface temperature is below saturation heat transfer is assumed to follow the well known relation

$$q'' = h_D (T_W - T_\ell) \quad ; \quad T_W \leq T_S \tag{B-1}$$

and we assume $h_D$ to be well represented by the Dittus-Boelter correlation. The coefficient for this relation is usually taken as

$$C_D = 0.023,$$

however, there is ample evidence ( , , ) that this value is dependent on the heating and flow geometries (inside tube, annullar, outside tube, etc.). We use the following data based values

$$C_D = 0.023 \quad \text{- heating inside tubes}$$
$$= 0.013 + 0.033\varepsilon \quad \text{- heating outside tubes} \qquad \text{(B-2)}$$

$\varepsilon$ = flow fraction of unit cell

Physically the heated surface will exhibit points of high free energy. Whether these are cracks with associated higher internal temperatures or simply sharp edges, a new mechanism may be assummed to come into play when the film temperature $T^* > T_s$. This mechanism will be referred to as the boiling heat flux and represented by $h_B (T_w - T_s)$. Thus the total heat flux is now taken as

$$q'' = h_D (T_w - T_\ell) + h_B (T_w - T_s) \qquad \text{(B-3)}$$

We do not assume that we switch correlations (as some do for example when $h_D (T_w - T_\ell) = h_B (T_w - T_s)$) but that there are two distinct mechanisms operative. Eq (B-3) defines the surface heat flux under all conditions of flow and void fraction as long as $T_w > T_s$. From a consideration of the data we believe $h_B$ is acceptably modeled by the Thom (_) correlation.

$$h_B = h_B^o (p) (T_w - T_s) \qquad \text{(B-4a)}$$

$$h_B^o (p) = 193e^{p/630} \quad \text{(English units)} \qquad \text{(304b)}$$

The reader will note the similarity to the Chen modeling where he takes (for $T_\ell = T_s$)

$q'' = (h_D F + h_{micro}) (T_w - T_s)$

If we compare with our model, take $F = 1$ and $h_{micro} = h_B$. Note that $h_{micro}$ is $\propto (T_w - T_s)^{0.99}$ hense the comparison

is quite close. Indeed if we plot $h_B/(T_w - T_s)$ and $h_{micro}/(\Delta T)^{.99}$ we have Fig. B-1. Since the Chen relation was developed for pressures below 500 psia (and most data was below 100 psi) and the Thom relation was optimized for pressures above 1000psia it apears reasonable to assume the Thom relation has a more general pressure dependence validity. Further, the calculation for the Chen coefficient (in Fig. B-1) does not include the S (Suppression) factor. There appears to us insufficient basis to the suggestion that voids stop forming at the wall simply because the flow gets high. Examination of the data appears as well to show bubbles still forming in the film even during the annular flow which presumable forms the basis for assuming the existance of suppression in the first place.* In any event the final model predicts rather accurate void fractions well into the annular flow regime (see Part 2).

While Eq (B-3) yields the total wall heat flux, we must still specify the separation into vaporization flux and bulk heating flux. When the B.L. temperature $T^* > T_s$ (implying $T_w > T_s$) any microscopic void formation on the wall has a potential for growth due to vaporization into it from the superheated B.L. Thus, the vaporization flux is taken as

$$q''_v = h_B(T_w - T_s) + h_D(T_w - T^*) \qquad (B\text{-}5)$$
$$= (h_B + \tfrac{1}{2} h_D)(T_w - T_s)$$

The bulk phase heating flux follows as

$$q'' - q''_v = h_D(T^* - T_\ell)$$
$$= \tfrac{1}{2} h_D (T_w - T_\ell + T_s - T_\ell) \qquad (B\text{-}6)$$

It is important to notice that $q'' - q''_v \not\rightleftharpoons 0$ as $T_\ell \to T_s$. This implies the liquid will superheat to some degree. This will be discussed in Appendix E. Note that the Reynolds number entering $h_D$ is taken as the liquid Reynolds

---

* R. Duffey, Private Communication

A COMPARISON OF THE THOM AND CHEN
MICRO-CONVECTION HEAT TRANSFER COEFFICIENTS

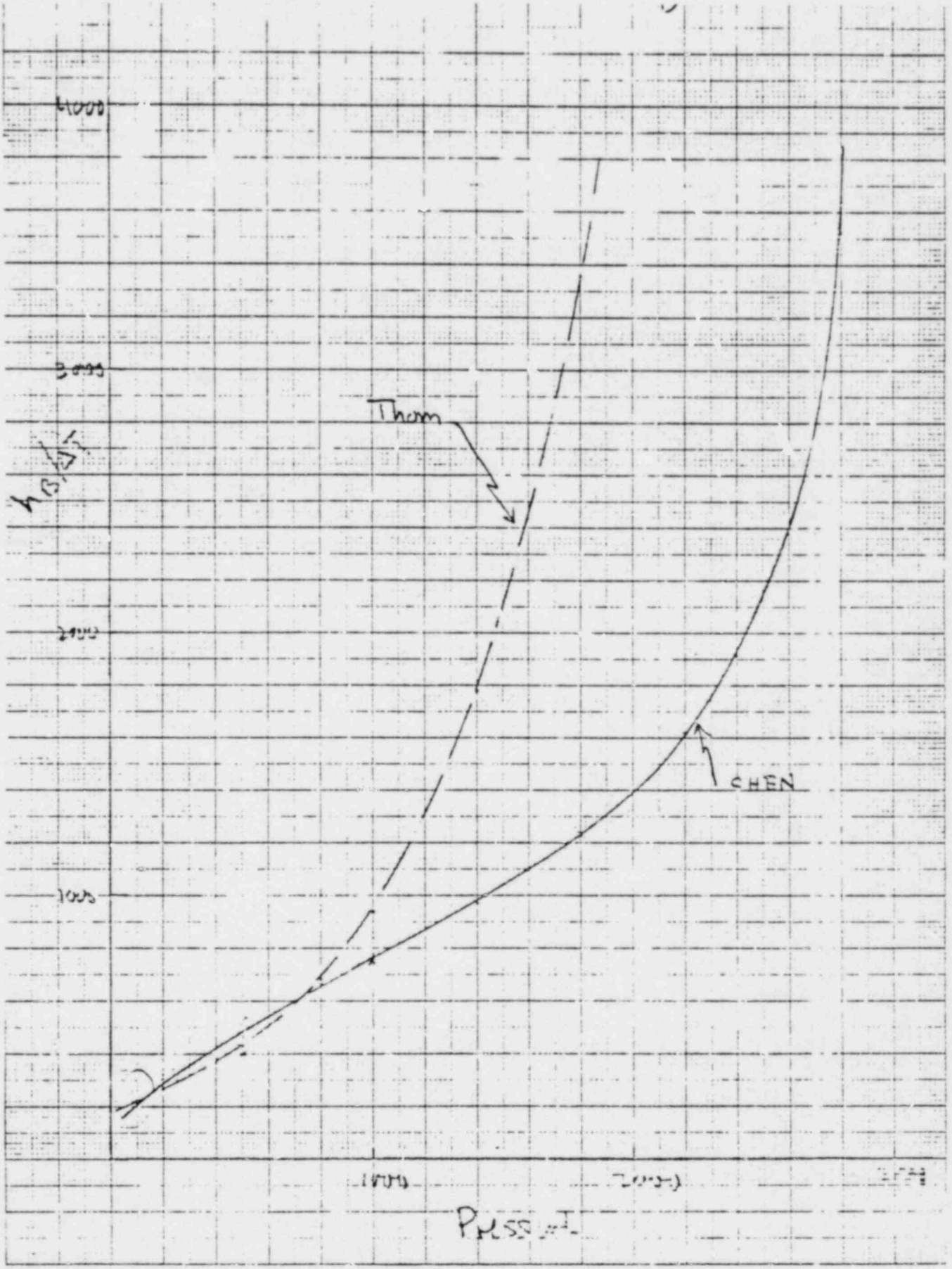


Fig. B1

number ($Re_\ell$) hence $h_D \to 0$ as the void fraction $\to 1$. In this report we do not include heat transfer directly to the vapor.

2. Void Formation in the Film

Although there is a potential for void formation when $T_w > T_s$ the subcooling of the bulk precludes significant void formation until some later distance down the heated channel. Indeed there is a near wall condensation potential acting (just as there is a boiling potential) and we take this potential as:

$$q''_C = h_A (T_s - T_\ell) \tag{B-7}$$

and net void formation would depend on whether $q''_V \lesseqgtr q''_C$ (see eq A4c). The literature contains a number of potential candidates for $h_A$; we have chosen the Hancox-Nicol (H & N) relation

$$h_A = C_A Re_\ell^{.662} \; Pr \; K_\ell/D_R \tag{B-8}$$

In this formulation H & N correlated the data based on circular tube experiments and inlet conditions. We have expanded the formulation to local conditions, a different voidage model and other geometries. Because of this we have optimized the coefficient (see Part 2):

$$C_A = 0.2 \text{ for tubes}$$
$$= 0.1 \text{ for other geometries} \tag{B-9}$$

We have also defined the diameter entering the Nussalt number to be the heated rod diameter ( = $D_e$ for tubes)

3. Direct Heating of the Liquid Phase

The $\gamma$ and inelastic neutron scatter in the liquid comprise a form of bulk heat generation. We take the deposition to be related to the average bulk phase density hence

$$q_v''' = (1 - \alpha) n P \qquad \text{(B10a)}$$

where P is the total power generation in the rod and n accounts for the fraction of energy escaping the rod and the inelastic scattering phenomena. We assume that for this form of energy deposition voids form directly (as microscopic bubbles). In other forms of bulk heating this may not be correct.

4. Bulk Condensation

In Appendix A we have introduced a bulk condensation term

$$q_c''' = h_c \left(\frac{A}{V}\right)_c (T_s - T_\ell) \qquad \text{(B10b)}$$

This condensation term is considered different from that leading to eqs B(7,8). That phenomena can be related to thelocation of the point of net vaporization and is not unrelated to surface condensation (the "surface" being the subcooled liquid interfacing the thermal boundry layer), while here we deal with the bulk void surface itself.

The following analysis starts with the single bubble model of Sursock and Duffey (_) and goes on to develop a formulation for $HA/V)_c$ (c.f. eq A-7) which does not contain sirgle bubble parameters. In the end we cannot utilize the result because of a lack of data necessary to evaluate the proportionality constant (at least we are unaware of any such data). Thus, it is unclear that the $\dot{r}_{g2}$ term (eq A-7) is currently usable in the subcooled flow regime unless one makes additional assumptions (instantaneous condensation, i.e., q"' heats the liquid phase directly).

Consider the condensation of a bubble. Following Sursock and Duffey we take for the individual condensing bubble

$$\frac{dR}{dt} = - \frac{k_T (T_s - T_\ell)}{(\rho_g h_{fg}) \sqrt{\frac{\pi k_T t}{\rho_\ell c_p}}} \qquad \text{(B-11)}$$

hence assuming that the bubble condenses completely

$$R^2 (0) = \frac{12 \rho_\ell c_p k_T}{\pi} \left( \frac{\Delta T}{\rho_g h_{fg}} \right)^2 t_c = \Theta t_c \qquad \text{(B-12)}$$

Eq. (B-12) actually defines $t_c$.

From thermodynamic considerations we can estimate the change of temperature of the liquid phase due to vapor condensation as

$$\Delta\alpha V = \frac{4}{3} \pi ( \Theta t_c)^{3/2} = \frac{(1 - \alpha) \rho_\ell c_p (T_\ell^* - T_\ell) V}{\rho_g h_{fg}} \qquad \text{(B-13)}$$

We now make assumptions concerning initial bubble size which may be valid for energy deposition from $\alpha$- rays and inelastic scatter which are probably not fully valid in other cases. We assume all initial bubble sizes are essentially the same and that the direct deposition void fraction is only a fraction of the local (cross section average) void fraction. In this case eq. (B-13) holds for many bubbles.

Consider now

$$T_\ell^* - T_\ell = (T_s - T_\ell) - (T_s - T_\ell^*) > 0$$

If $T_\ell$ is the bulk temperature that would exist without direct bulk vaporization then $T_\ell^* - T_\ell$ must be proportional to the amount of such voidage actually condensed. Hence we take (approximately)

$$T_\ell^* \approx T_\ell + \frac{\int_0^z h_c\left(\frac{A}{V}\right)_c (T_s - T_\ell)\, dz}{G_\ell c_p} \qquad \text{(B-14)}$$

hence

$$T_\ell^* - T_\ell \approx \overline{h_c\left(\frac{A}{V}\right)_c (T_s - T_\ell)} \; \frac{z}{G_\ell c_p}$$

and we assume as well

$$\overline{h_c \left(\frac{A}{V}\right)_c (T_s - T_\ell)} = \overline{h_c\left(\frac{A}{V}\right)_c} \; (T_s - T_\ell)$$

with these we may write

$$\frac{4}{3}\pi (\Theta t_c)^{3/2} = \frac{(1-\alpha)\rho_\ell \; z(T_s - T_\ell)}{\rho_g h_{fg} G_\ell} V h_c \left(\frac{A}{V}\right)_c \qquad \text{(B-15)}$$

$$= \gamma V h_c\left(\frac{A}{V}\right)_c$$

From eq. B-12 we can determine the area per unit volume of a bubble (hence by the above assumptions of the mass of bubbles)as

$$\left(\frac{A}{V}\right)_c \approx 4\pi \left(\frac{3}{4\pi} \gamma V\right)^{2/3} h_c \left(\frac{A}{V}\right)_c^{2/3}$$

hence

$$\left(\frac{A}{V}\right)_c \approx (4\pi)^3 \frac{\left(\frac{3}{4\pi}\gamma V\right)^2}{V^3} h_c^2 \qquad \text{(B-16)}$$

During conduction controlled vapor condensation across a convective boundry layer the heat transfer coefficient can be represented as

$$h_c = k_\ell / d$$

with $d \propto \sqrt{t_{cps}\, k_\ell / c_p \rho_\ell}$

and the time to collapse given by

$$t_{cps} \propto R(0) \,/\, |v_g - v_\ell|.$$

Using eq. (B12, 15)

$$d \propto \sqrt{\frac{k_\ell \left(\frac{3}{4\pi}\gamma V h_c \left(\frac{A}{V}\right)_c\right)^{1/3}}{c_p \rho_\ell |v_g - v_\ell|}}$$

hence

$$h_c \propto \sqrt{\frac{k_\ell \rho_\ell c_p |v_g - v_\ell|}{\left(\frac{3}{4\pi}\gamma V \frac{h}{\left(\frac{A}{V}\right)_c}\right)^{1/3}}} \qquad \text{(B-17)}$$

If we multiply eq (B-16) by $h_c$ and substitute the cube of eq (B-17) on the right hand side, we find after some cancellation:

$$h_c \left(\frac{A}{V}\right)_c = (36\pi)^{2/3} C_c \frac{c_p \rho_\ell}{\rho_g h_{fg} D_e} | S - 1 | \frac{z}{L} (T_s - T_\ell) k_\ell / D_e \qquad \text{(B-18)}$$

where we have assumed $V \propto D_e^2 L$. This result can be cast into the form

$$h_c \left(\frac{A}{V}\right)_c = \bar{C}_c \, Ja \, | S - 1 | \, z k_\ell / D_e^2 \, L$$

hence the condensation Nussult number can be taken as

$$\frac{D_e^2 h_c}{k_\ell} \left(\frac{A}{V}\right)_c \equiv (Nu)_c = \bar{C}_c \, Ja \, | S - 1 | \, z/L$$

The final result is that bulk condensation is proportional to $(T_s - T_\ell)^2$ as found by Sursock and Duffey for the single bubble but all single bubble parameters have been eliminated.

The analysis permits us to specify $q'''_c$ within a constant multiplier but the extant data on bulk condensation appears insufficient to estimate a value for this constant.

## APPENDIX C

## Slip Modeling

In the origional model established in 1972 (__) the slip relation was taken as a slight modification of the Bancoff-Jones model

$$S \equiv \frac{v_g}{v_\ell} = \frac{1 - \alpha}{\kappa(\alpha,p) - \alpha} \tag{C-1}$$

with

$$\kappa(\alpha,p) = \kappa_1 + (1 - \kappa_1)\alpha^{r(p)} \tag{C-2}$$

$$\kappa_1 = 0.71 + 0.29\ p/p_{CR}$$

$$r(p) = 3.448275 - (1.875 \times 10^{-4} - 5.85 \times 10^{-7} p)p$$

As was noted then this formulation has several desirable properties.

- $S \to 1$ for $p \to p_{CR}$ for all $\alpha$
- $S \to \infty$ for $p \to 0$ at $\alpha = 1$

The rationale for these "desired" properties was: (1) for $p \leq p_{CR}$ we cannot differentiate between the phases hense $S \to 1$ for all $\alpha$, (2) since the vapor specific volume is infinite at $p = 0$ any voidage should lead to $\alpha = 1$ and $S \to \infty$. We commented that this implied that $\alpha$ was somehow related to $\rho_\ell/\rho_g$ as had been pointed out by Achmed. We also noted that when the bubble leaves the wall it starts with zero velocity, hence S should go to 0 as $\alpha \to 0$ for all p, but eq (C-1) did not exhibit this property. We suggested however that this could be achieved if $\kappa(\alpha,p)$ was replaced by $\kappa(\alpha,p)/L\ (\alpha,p)$ where

$$L(\alpha,p) = \frac{1 - e^{-c_1(p)\alpha}}{1 - e^{-c_1(p)}} \tag{C-3}$$

with

$$C_1(p) = C_1^c p_{CR}^2 \;/\; \left(p(p_{CR} - p)\right)$$
$$C_1^o = 4.4$$

There has been a great deal of work done on the subject of slip and we have attempted to synthesize a model which contains the features observed in experiment and is valid in vertical geometries. We start with a Zuber-Findley drift flux model

$$v_g = C_o\,(\alpha v_g + (1 - \alpha)\, v_\ell) + v_{g\ell}(\alpha) \qquad \text{(C-4)}$$

The terms in eq (C-4) are cross section averages; if $< >$ implies such an averaging then

$$v_g \equiv \langle \alpha v_g \rangle / \langle \alpha \rangle$$

$$\alpha \equiv \langle \alpha \rangle$$

$$C_o \equiv \frac{\langle \alpha(\alpha v_g + (1 - \alpha) v_\ell) \rangle}{\langle \alpha v_g + (1 - \alpha)\, v_\ell \rangle \langle \alpha \rangle}$$

$$v_{g\ell}(\alpha) \equiv \frac{\langle \alpha(1 - \alpha)\,(v_g - v_\ell) \rangle}{\langle \alpha \rangle}$$

Equation (C-4) can be rearranged to yield

$$S \equiv \frac{v_g}{v_\ell} = \frac{1 - \alpha}{1 - C_o \alpha}\left[C_o + \frac{\rho_\ell\, v_{g\ell}(\alpha)}{G_\ell}\right] \qquad \text{(C-5)}$$

Starting with eq (C-5) we must fit all of the physics into $C_o$ and $v_{g\ell}(\alpha)$. There are several conditions which a ratio of the phase velocities must meet:

C1 $\lim_{p \to p_{CR}} S(\alpha,p) = 1$

C2 $\lim_{p \to o} S(1,p) = \infty$

C3 $S(\alpha,p)$ finite except for C2

C4 $\lim_{\alpha \to 0+} S(\alpha,p) = v_{g\ell}(0)/v_{\ell} > 0$

There are also a number of experimental observations

O1 $C_o$ depends on mass flow

O2 $C_o$ depends on pressure

O3 $C_o$ depends on void fraction

O4 $C_o$ and $v_{g\ell}(\alpha)$ depend on flow geometry (e.g. equivelent diameter)

O5 $v_{g\ell}(\alpha) \propto (1 - \alpha)^b$

These are not the only possible conditions or observations Premoli et al (_) list 7 conditions on S relating to $D_e$, $G_o$, $\mu_{\ell}$, and $\sigma$, none of which we would fully agree with. We have not listed any dependance of $C_o$ or $v_{g\ell}$ on flow regime (flow maps) although various analyses have shown specific limits to which $C_o$ or $v_{g\ell}$ must tend if one had a fully developed invarient regime of a specific type. As with the heat transfer coefficients we aschew maps because of the jump phenomena associated with boundry crossing and because no extant flow map is--to our knowledge--demonstrably valid in any specific

situation. As is shown in Part 2 of this report flow maps are not needed to achieve excellent comparison with data.

From the observations we may determine the characteristics of $C_o$ and $v_{g\ell}$ needed to satisfy the conditions C1 - C4.

Condition C-1

$$\lim_{p \to p_{CR}} S(\alpha,p) = 1$$

from eq. C-5 this implies

$$C_o \longrightarrow 1 - (1 - \alpha)\, v_{g\ell}\, \rho_\ell / G_\ell$$

but, $v_{g\ell}$ is a measure of buoyancy hence $v_{g\ell} \to 0$ as $p \to p_{CR}$ and C1 implies $\lim_{p \to p_{CR}} C_o \longrightarrow 1$ for all $\alpha$

Condition C-2

$$\lim_{p \to 0} S(1,p) = \infty$$

Since $S(1-\epsilon,p) = \dfrac{\epsilon}{1 - C_o + C_o\epsilon} \qquad \left[C_o + \text{etc.}\right]$

and the numerator of $S \to 0$ as $\epsilon \to 0$ we must require $1 - C_o + C_o\epsilon \to 0$ as $\epsilon \to 0$. Hence C2 also implies

$$\lim_{\alpha \to 1} C_o \to 1$$

and this yields $S \to \dfrac{0}{0}$

Expand eq (C-5) use 05 and L' Hopitals rule to yield

$$\lim_{\alpha \to 1} S = \lim_{\alpha \to 1} \frac{1}{\frac{1-d(1/C_o)}{d\alpha}} + \frac{b\,(1-\alpha)^{b-1}\, v^{o}_{g\ell}/v_{\ell}}{1 + \frac{dC_o}{d\alpha}}$$

where $v^{o}_{g_\ell}$ is the $\alpha$ independent part of $v_{g\ell}$ and $v_{\ell}$ is not differentiated here. For C-2 to hold $\lim_{\alpha \to 1} \frac{d\ 1/Co}{d\alpha} \to 1$. Note that the second term is still in an indetermanent form (0/0) but if b > 1 then the first term dominates*, i.e.

$$\lim_{\alpha \to 1} (1 + b(1 - \alpha)^{b-1}\, v^{o}_{g\ell}/v_{\ell}) = 1$$

## Condition C-3

S $(\alpha,p)$ finite except for C2 implies

$$\frac{1}{C_o} \geq \alpha$$

and that the equality can only occur for $\alpha = 1$, $p = 0$.

## Condition C-4

C-4 states simply that we are dealing with co-current flow and that the initial slip ratio is not zero but has the buoyancy value. It also implies that the vapor bubbles initially start rising in the superheated boundry layer since C-4 also can be read as

---

* It actually doesn't matter if b = 1 the value for S is still infinite as $\alpha \to 1$.

$$\lim_{\alpha \to 0+} S \longleftrightarrow \lim_{\alpha \to 0+} C_o = 0$$

The four conditions on the slip ratio may be replaced by equivelent conditions on $C_o$ and $v_{gf}$:

$$\lim_{p \to p_{CR}} C_o = 1 \text{ for all } \alpha > 0 \tag{C6a}$$

$$\lim_{\alpha \to 0} C_o = 0 \tag{C6b}$$

$$\lim_{\substack{\alpha \to 1 \\ p \to 0}} \frac{dC_o}{d\alpha} = 1 \tag{C6c}$$

$$\lim_{\substack{\alpha \to 1 \\ p \to 0}} b \geq 1 \tag{C6d}$$

$$\frac{1}{C_o} \geq \alpha \tag{C6e}$$

Consider the following form for $1/C_o$.

$$\frac{1}{C_o} = \left(\kappa_1(p) + \left(1 - \kappa_1(p)\right)\alpha^{r(p)}\right) / L(\alpha, p) \tag{C-7}$$

If $r(p) \geq 0$ and $\kappa_1(p) \geq 0$, eq. (C-6a) is automatically satified if

$L(\alpha,p_{CR}) = 1$ and Eq. (C6b) is replaced by

$$\lim_{\alpha \to 0} \quad L(\alpha,p)=0 \qquad \text{(C-6b)}$$

Eq. (C-6c) implies

$$\lim_{p \to 0} \quad \frac{L(1,p)\, r\,(p)\,(1-\kappa_1) - \left(\frac{dL}{d\alpha}\right)_{\alpha=1}}{L^2\,(1,p)} \quad = \quad 1 \qquad \text{(C-8)}$$

Consider the $L(\alpha,p)$ function. It is introduced to account for the observations that bubbles formed near the wall tend to have slip values < 1, and conceptually at least a bubble when it breaks off the wall should start off with zero initial velocity (although we choose here to take the acceleration time to terminal velocity small, hence take $v_{g\ell}(0)$ as its asymptotic value). Also we know that these near wall effects are limited to small values of the average void fraction, hence that $L(\alpha)$ should have only a weak $\alpha$ dependance for $\alpha$ greater than a very few tenths. We choose the form for $L(\alpha)$ as

$$L(\alpha,p) \quad = \quad \frac{1 - e^{-c_1(p)\alpha}}{1 - e^{-c_1(p)}} \quad , \qquad \text{(C-9)}$$

which satisfies eq (C-6b'). Returning to eq (C-8) we see that eq (C-9) implies

$$\lim_{p \to 0} \quad \left\{ r(p)\,(1-\kappa_1) \quad \frac{c_1(p)\, e^{-c_1(p)}}{1 - e^{-c_1(p)}} \right\} \quad = \quad 1$$

Now with the above definition of $L(\alpha,p)$ we can only have $L(\alpha, p_{CR}) = 1$ for all $\alpha > 0$ if $c_1 \propto \frac{1}{p_{CR} - p}$ $(p \leq p_{CR})$. We choose now

$$c_1(p) \propto \frac{p_{CR}^2}{p(p_{CR} - p)} \qquad \text{(C-10)}$$

This form eliminates the $C_1$ term in the zero pressure limit and we have

$$\lim_{p \to 0} \quad r(p) \left(1 - \kappa_1(p)\right) = \quad 1 \qquad \text{(C-11)}$$

Quite generally since $S \lesssim 0$ we must require eq. (C-6e) hold for all p and this basically

$$1 - r\,(p)\,(1 - \kappa_1) + \frac{\tau_1(p)\, e^{-c_1(p)}}{1 - e^{-c_1(p)}} \quad \gtrsim \quad 0$$

for all p. Although the last term assists in satisfying the inequality we shall end up with a constant of proportionality of about 4 (See Part II) hence the final term is quite small; basically we require

$$r\,(1 - \kappa_1) \; < \; 1 \qquad \text{(C-12)}$$

The original determination of r by Jones led to

$$r(p) = 3.53125 - 0.1875 \left(\frac{p}{1000}\right) + 0.58594 \left(\frac{p}{1000}\right)^2$$

We adjusted this to the p = 0 limit of

$$r(0) = 3.448275$$

in order to avoid negative slip below about 50 psi. Basically this r value is 1/0.29. If we extract the r(0) value and rescale to $p_{CR}$ we found

$$r(p) = \frac{1}{0.29} \left[1 - 0.1743\left(\frac{p}{p_{CR}}\right) + 1.746 \left(\frac{p}{p_{CR}}\right)^2\right]$$

The simplicity of this form led to an examination of whether this polynomial could be replaced by one based on the thermodynamic variables. The final choice was

$$r(p) = \frac{1}{0.29} \qquad (1 + 1.57\ \rho_g / \rho_\ell)$$

Although the initial slopes (around p = 0 ) are distinctly different the overall curves are quite close. Consider also a form for $\kappa_1$

$$\kappa_1(p) = \kappa_o + (1 - \kappa_o)\ (p/p_{CR})$$

This form is similar to that used in (_) and was proposed by Jones. As above we replace $p/p_{CR}$ by a (nearly) equivelent function of $\rho_g/\rho_\ell$ and take (see Part II)

$$\kappa_1(p) = \kappa_o + (1 - \kappa_o)\ (\rho_g/\rho_\ell)^{\frac{1}{4}} \qquad \text{(C-13)}$$

with this choice

$$r(p) = \frac{1}{1 - \kappa_o}\left[1 + 1.57\ \rho_g/\rho_\ell\right] \qquad \text{(C-14)}$$

This does indeed satisfy eq (C-12) for all p. Indeed all conditions are satisfied except for eq (C-6d).

## The Drift Velocity

Equation (C-4) is written as an equality. In fact, however, it is an identity and contains no information as such. The term $v_{g\ell}$ contains as much information as all of eq (C-4) if one could but write a relation for it. Indeed this has been done a number of times ( , , ,) for well characterized flow regimes. Ishii for example has derived a number of analytical forms for annular flow which contain terms proportional to $(1 - \alpha)^3$ and $(1 - \alpha)^2$, but his definition for $v_{g\ell}$ appears to be different from ours. Although it is annoying, there are a number of ways that the identity between average vapor and liquid velocity can be written, Malnes discusses three, for our purposes the specific original form of $v_{g\ell}$ is not of im-

portance since we have not proposed to try to determine analytic forms for $C_o$ or $v_{g\ell}$ but ultimately to fit the terms through the use of data. Thus, we apriori assume that eq (C-4) is an equality and attempt to fit $C_o$ and $v_{g\ell}$. We assume that $v_{g\ell}$ is a measure of buoyancy in the low $\alpha$ limit and take

$$\lim_{\alpha \to 0} v_{g\ell} = C_2 \left[ \frac{(\rho_\ell - \rho_g)}{\rho_\ell^2} \sigma g g_c \right]^{1/4} = v_{g\ell}^{\circ} \qquad \text{(C-15)}$$

If we use the definition flow quality $X \equiv G_g/G_o$ and we remember that $G_o = G_g + G_\ell$ then we may write

$$\alpha \equiv \frac{X}{X + \frac{\rho_g}{\rho_\ell} S (1 - X)}$$

hence using eq (C-5) we find

$$X = \frac{\alpha \rho_g/\rho_\ell \left( C_o + \frac{v_{g\ell} \rho_\ell}{G_o} \right)}{1 - C_o \alpha + C_o \alpha \rho_g/\rho_\ell} \qquad \text{(C-16)}$$

As $\alpha \to 1$ we observe that

$$X \longrightarrow 1 + v_{g\ell} (1) \rho_\ell/G_o$$

and since X must $\to$ 1 as $\alpha \to 1$ we have

$$\lim_{\alpha \to 1} v_{g\ell} = 0$$

and

$$v_{g\ell} \propto (1 - \alpha)^b \text{ with } b > 0$$

Which along with condition C3 leads to eq (C-6d) and

$b \geq 1$

Since the slip should not be bouyancy dependent as $\alpha \rightarrow 1$ we choose (finally)

$$b = 3/2 \qquad \text{(C-18}$$

which is related to single bubble behavior. The coefficient $C_2$ is taken from the literature ( ) as

$$C_2 = 1.41 \qquad \text{(C-19)}$$

The parameter $\kappa_o$ is the only one that has not been determined and we use it to introduce mass flow dependance.

It has been observed that $C_o$ has a limiting value of 2 in laminer flow in tubes; we introduce this observation through an approximate relation

$$1/\kappa_{o1} = 1 + e^{-Re/10^5} \qquad \text{C-20}$$

where Re is taken as the inlet value using $G_o$ and defining D as $D_{HY}$. Numerical studies however show that for large values of Re $\kappa_{o1}$ becomes too large and we find it necessary to apply a cut off on Re such that

$$\kappa_o = \min \left\{ \kappa_{o1}, \kappa_{o2} \right\} \qquad \text{(C-21)}$$

where

$\kappa_{o2}$ = 0.8 for cylinders, annulli and bundles

= 0.71 for channels

It is clear that this development will not satisfy all readers. The slip defined here is monotonic with $\alpha$ and does not peak; the very low flow values are probably incorrect because $v_{g\ell}$ does not contain a strong diameter dependence (only through $\kappa_o$). However, the general quality of the predictions are such as to make this slip model acceptable for its desired uses: relatively high flows and pressures above a very few hundred psi.

## APPENDIX D

### Location of the Point of Net Vapor Generation (NVG)

The subcooled void formation model we establish and qualify is different from those in the literature and one of the adjustable parameters in the model is the condensation coefficient $C_A$ introduced in $\dot{\Gamma}_{g1}$. It is adjusted to secure a statistically good fit to the data and basically $C_A$ determines the point of NVG and we believe deserves further discussion. This location ($Z_D$) is often referred to as the point of void departure or detachment and we shall use the terms interchangably.

The location of $Z_D$ occurs where

$$Z_D = \text{Min} \left\{ Z_\alpha, Z_o \right\}$$

and $Z_\alpha$ is the axial location where $\alpha$ is the first non-zero,

and $Z_o$ is the axial location where $\dot{\Gamma}_g$ is first positive.

In steady state where the fluid enters subcooled $Z_D = Z_o$; however, during a transient reduction in power generation could lead to a situation where $\dot{\Gamma}_g < 0$ but $\alpha > 0$ in this case $Z_D = Z_\alpha$. When $Z_D = Z_\alpha$ we can usually expect some condensation to occur. In the usual experimental situations where $\eta P = 0$ we expect $Z_D = Z_o$.

Hence, by neglecting direct deposition and at steady state we have $Z_D$ defined as follows: when $\dot{\Gamma}_{g1} = 0$

$$q''(Z_D) = q''_{out}(Z_D) + h_A (T_S - T_\ell)$$

now using the definitions for q" (eq 2b) and $q''_{out}$ (eq A5) and first solving the energy equation up to the point of departure (NVG) we find

$$h_\ell(Z_D) = h_\ell(0) + \frac{4}{G_o D_e} \int_0^{Z_D} q''(Z)\, dz$$

from this we may determine the bulk temperature $T_\ell(Z_D)$ and two values for the wall temperature

$$T_{w1} = (q'' + h_D T_\ell + h_B T_s) / (h_B + h_D)^*$$

$$T_{w2} = T_s + 2q' - 2(h_A + h_D)(T_s - T_\ell)$$

The correct value for $Z_D$ is where $T_{w1} = T_{w2}$. This is in fact a fairly complex model for determining $Z_D$. Other authors have assumed that $Z_D$ is reached when the condensation term matches the total heat source, i.e. when

$$h_c \left(T_s - T_\ell (Z_D)\right) = q'' \qquad (D\text{-}2)$$

and $Z_D$ is found from $h_\ell (Z_D)$ (i.e. from the energy equation). In this form the wall temperature (hence the wall superheat) does not appear at all. We believe this lack is a serious one since the wall superheat is a basic determinant for subcooled void formation. The statistical analyses of Part II shows that the $h_A$ correlation of Hancox and Nicol (with a change in $C_A$) predicts not only the point of detachment quite nicely but the subcooled model $\dot{\Gamma}_g$ allows an accurate prediction of the void fraction in the rest of the subcooled regime as well.

If one were to try to compare the earlier correlations of Saha and Hancox and Nicol (H & N) with the present one then we should have to define a pseudo coefficient

$$h^* = h_D + h_A \left[\frac{h_B + h_D}{h_B + \tfrac{1}{2}h_D}\right] ;$$

The fact that $h_B \propto T_w - T_s$ does not impact here since the $h_A$ multiplier must lie between 1 and 2 hence a simple range for h* can be determined. One can now create a simple plot of the critical Stanton number at detachment

---

* Since $h_B = h_B^\circ (T_w - T_s)$ $T_{w1}$ is realy solved for from a quadratic equation

versus Paclet number. The definitions imply

$$St = Nu/Pe$$

$$= \frac{h}{kPe/D}$$

Where h is any of the correlations being considered. In this form

$$q'' = h\left(T_s - T_\ell(Z_D)\right)$$

as for Saha but h* depends directly on the wall superheat. If we take the Saha data analysis ( ) and show it along with the H & N and the present correlation we have the presentation in Fig. D-1. While the Saha data display covers the same range for the Peclet numbers generally of interest the trend of the present correlation is significantly different. Because of the degree of disagreement some further discussion appears warranted.

There are three points which appear of interest here, and they are:

- The definition of the point of vapor generation (PVG)
- The determination of the PVG from the experimental data
- The sensitivity of the prediction of the Stanton number to the inferred liquid subcooling

1. Defining the Point of Vapor Generation

Basically all researchers appear to be agreed that there is a region of quite low void fraction followed by one of more rapidly increasing void fraction and that where one ends and the other begins defines the point of net VG. Unfortunately the data usually does not have such labels attached to it. The current model defines a point of VG which (viz. Fig. ) often exhibit long,low void fraction tails. It is not clear then that the current model defines the same point of departure as other models do.

2. Determining PVG from Experimental Data

A determination fo the PVG from the experimental data is necessary in

A COMPARISON OF
THREE HEAT TRANSFER CORRELATIONS
FOR
PREDICTING DETACHMENT

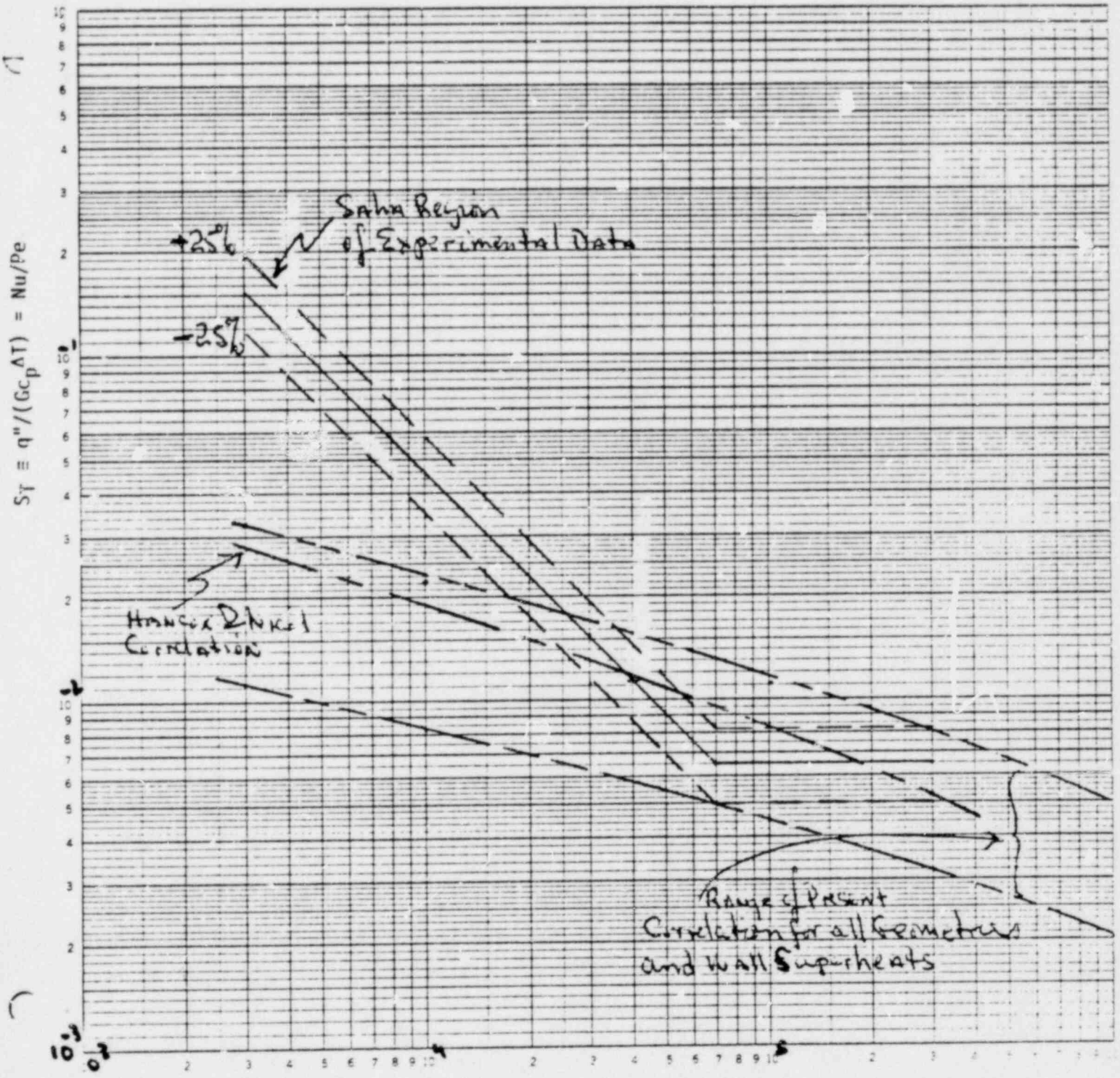


Fig. D1

$Pe \equiv GDc_p/k \equiv RePr$

order to determine the liquid subcooling at that point. In order to demonstrate the difficutly of getting a reasonably clear estimate we have re-examined several sets of experimental data of void fraction versus heated length (Fig. 3-8). We have tried to determine the minimum and maximum values for the location of PVG that could reasonably be inferred from the data in order to place error bars on the subsequent determination of the Stanton number. The results are shown in Fig. 2. The single symbol points are relatively cleanly determined as far as the published data is concerned while the others exhibit significant error bars. It is not clear that this presentation of data supports the S.Z. data range. Other data points due to Egan and Ferrell are also shown with extimates of the location of the PVG based on the steepest slope of void fraction versus distance and on a less steep projection (the circled crosses in Fig. 8).

3. The Prediction of the Stanton Number

The procedure we have used in determining the St,'Pe data space is quite straightforward. Thus if

$$\Delta T_D \equiv T_s - T_\ell (Z_D)$$

$$\Delta T_{sub} \equiv T_s - T_\ell (0)$$

then

$$S_T \equiv q''/G c_p \Delta T_D \qquad (17a)$$

$$Pe \equiv GD c_p / k$$

and if q" is constant

$$\Delta T_D = \Delta T_{sub} - (S_T \cdot \Delta T_D) 4Z_D/De \qquad (17b)$$

Since $(S_T \cdot \Delta T_D)$ is defined as $q''/Gc_p$ it is possible to secure $\Delta T_D$ (hence $S_T$) if $Z_D$ is known. Interestingly several experimenters have assumed

THE EFFECT OF ERROR BARS OF THE LOCATION OF
THE POINT OF NVG ON THE SAHN-ZUBER DATA DISPLAY

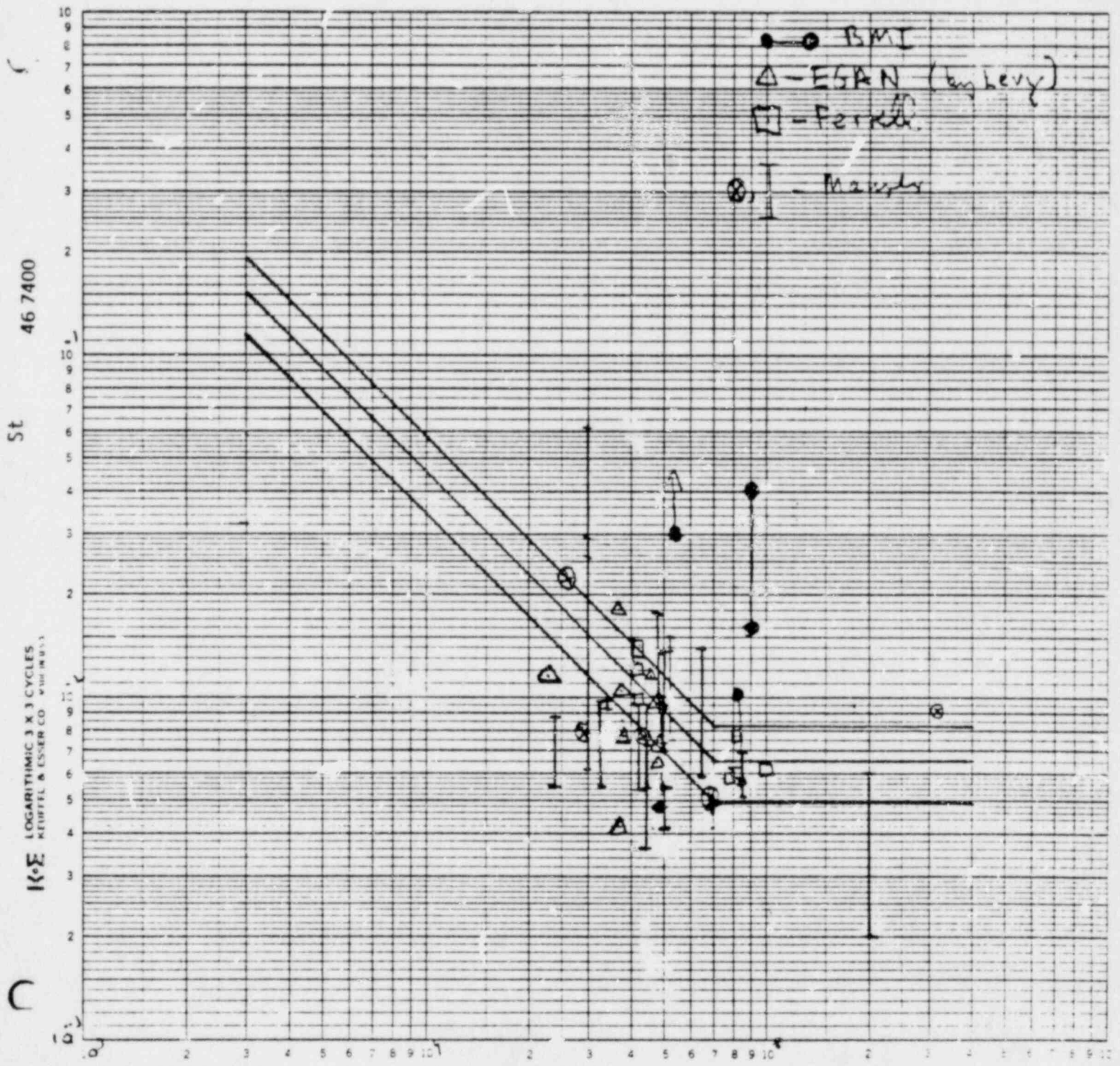


Fig. 2

Pe

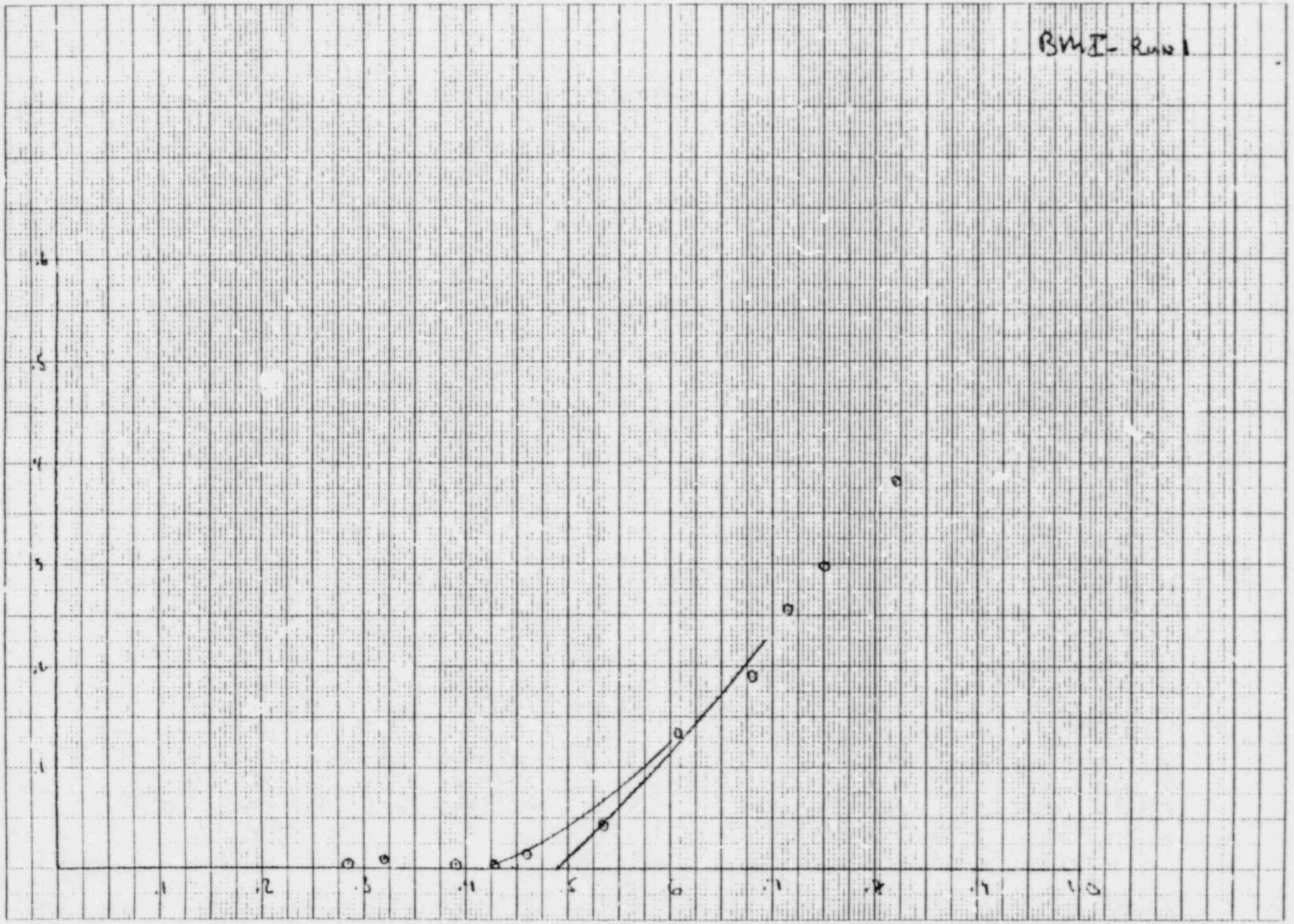
BMI- Run 1
.6
.5
.4
.3
.2
.1

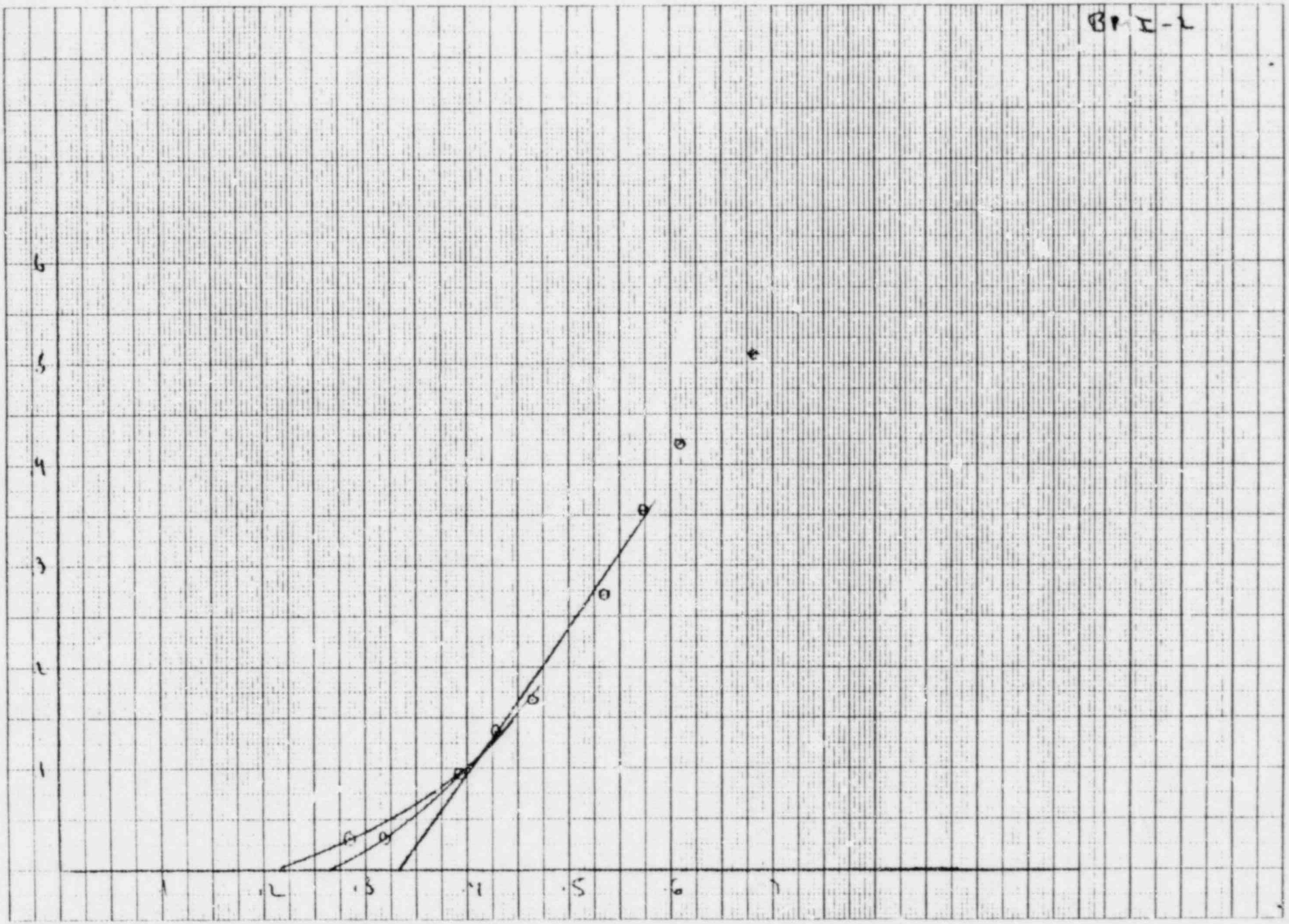


Fig. 4

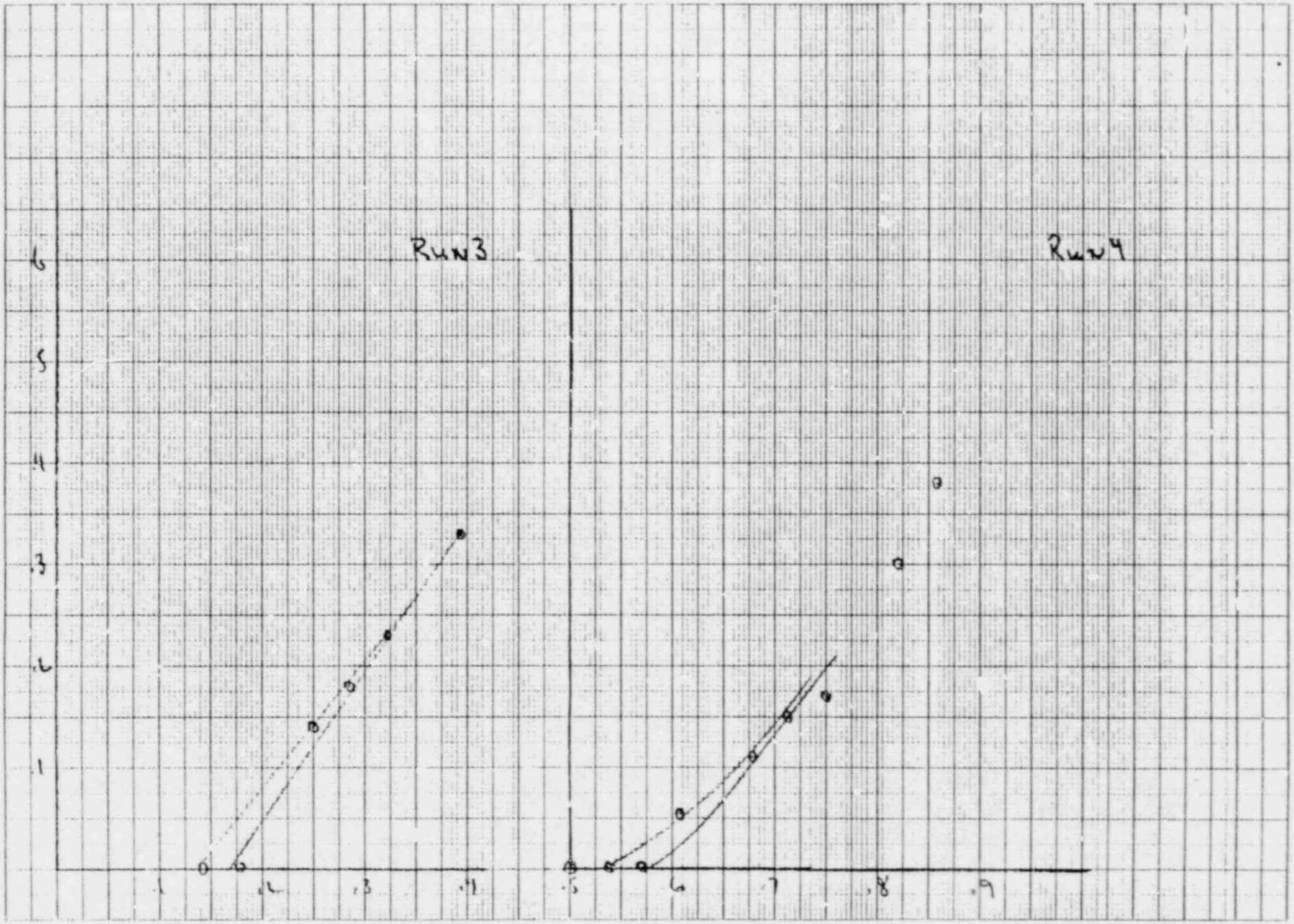


Fig. 5

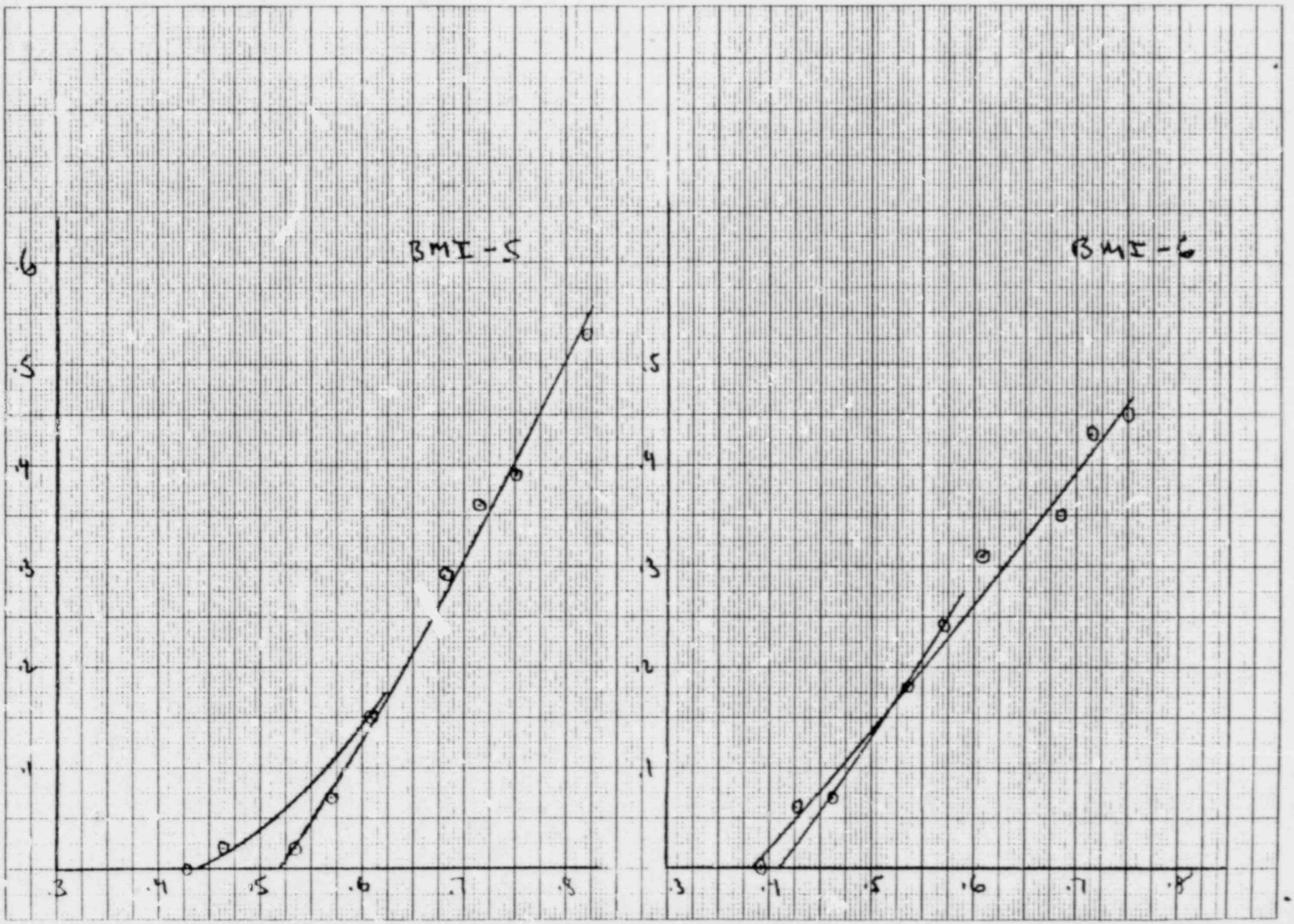


Fig. 6

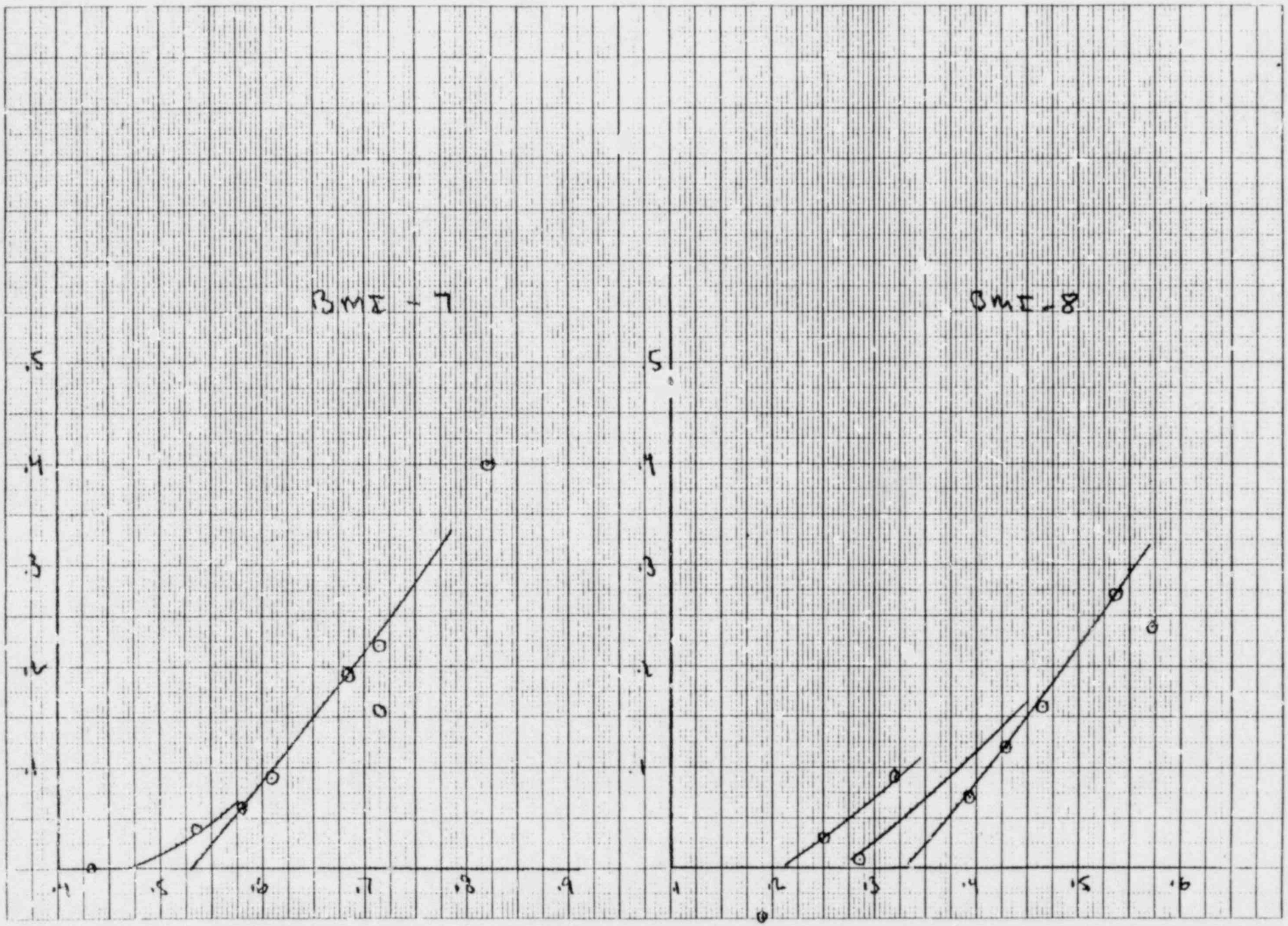
BMI - 7
BMI - 8

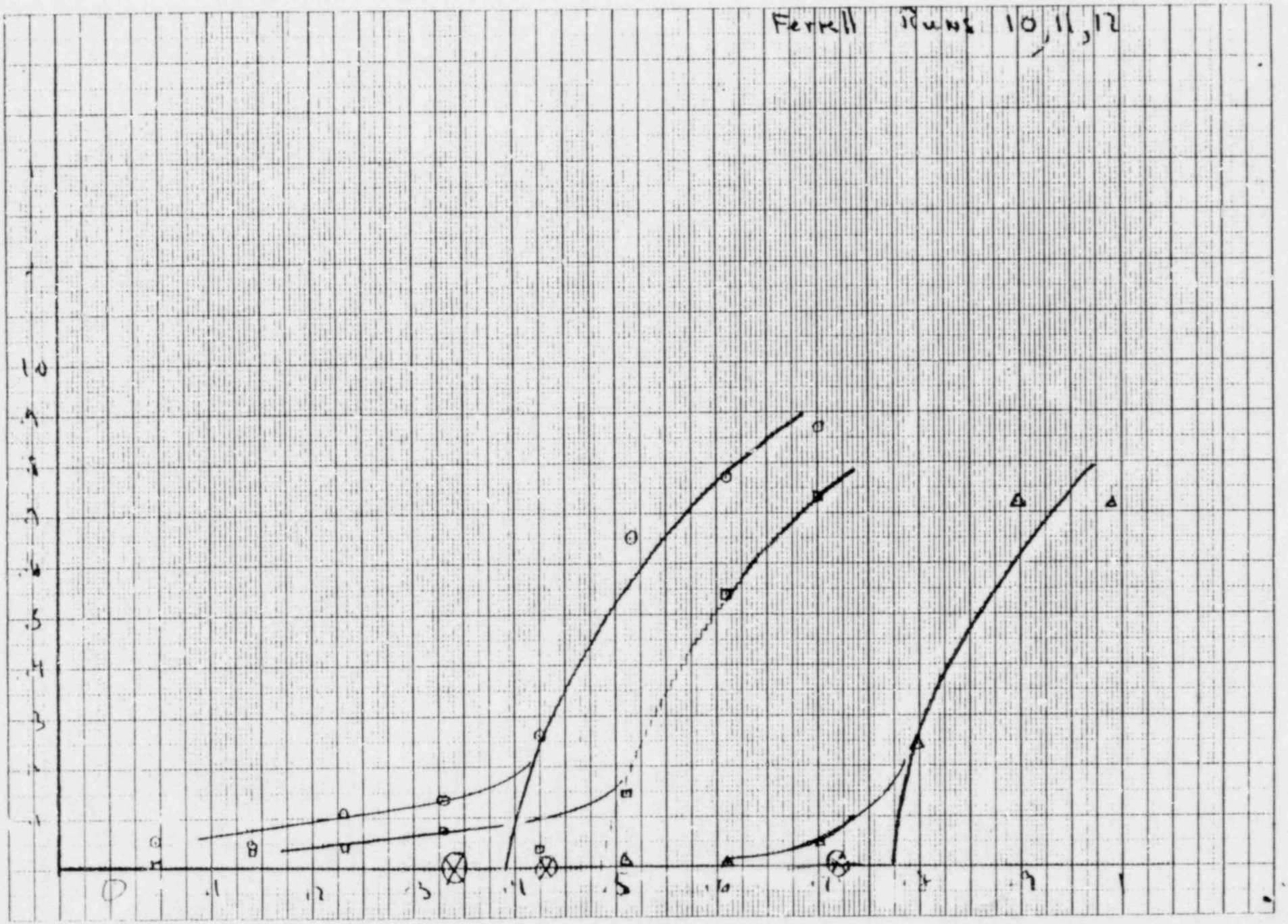


Fig. 8

that the point of vapor generation is given by continuing the line of maximum slope of $\alpha$ versus $Z$, or $\alpha$ versus $X_{eq}$ down to the abcissa; the intersection then defines the departure point. In Fig. 3-8 we show some of the Foglia and Ferrell data along with what we feel are reasonable estimates of the point of void departure. In many cases the difference is not significant while in others (Fig. 8) it can lead to large changes in the calculated value of $\Delta T_D$. Using Fig. 8 as an example, we find the reported value of $\Delta T_D$ to be 23 F (for each of the cases) while the calculated values range from 13-46 depending of which run is used and which intercept is considered "reasonable". Thus the Stanton number calculated from the $\Delta T_D$ can have considerable variation and exhibits, we believe, a wider scatter than is evident from the S-Z data display.

We believe in fact that the usual difinition of PVG may be counter-productive. The effects of tails may be quite significant (due to reactivity feedback effects) in application of models and their neglect may not be acceptable. Because of this we believe that the actual PVG is less important than the statistical agreement between data and prediction above some small value of void fraction (say 1 - 2%). The adequacy of the current model is established in this way.

## Appendix E

## Bulk Phase Superheating

The reader will note that although source terms may change with differing flow regimes they are continuous across flow regimes. This is true with the exception of the cross-over from subcooled to saturated conditions. We have shown that $q''_{out} \not\longrightarrow 0$ as $T_\ell \longrightarrow T_s$ hence that there must either be a jump in $\dot{\Gamma}_g$ or we must allow the bulk phase to superheat. The reader may suspect that had $q''_{out}$ been proportional to $T_s - T_\ell$ (instead of $T^* - T_\ell$) there would have been a smooth transition to saturated condition with no jump and no superheating of the bulk phase. That conclusion would however have been incorrect.

### Approaching Saturation Conditions

One of the difficulties(in our estimation) with earlier mechanistic models of flow boiling is that the source term for heating the liquid is usually proportional to $T_s - T_\ell$. In this situation we have as steady state (neglecting pressure effects):

$$G_\ell \frac{dh_\ell}{dz} = 4h (T_s - T_\ell) / D \qquad \text{(E-1)}$$

and from eq (E-1) it is clear that $T_\ell \longrightarrow T_s$ either when $G_\ell \longrightarrow 0$ or when $h_\ell \longrightarrow h_s$ (implying $\frac{dh_\ell}{dz} \longrightarrow 0$). The first implies $\alpha = 1$ and the second can occur only when $Z \longrightarrow \infty$. Neither of these is physically acceptable. We avoid them here by taking the bulk source term non zero as $T_\ell \longrightarrow T_s$ and are faced with the question of jumps or superheating.

This problem and conclusion is not characteristic of this model, or even of one dimensional models, nor does it go away if we include pressure

effects. It is fundamental. Thus if after $T_\ell = T_s$ $\dot{\Gamma}_g = q_{total}/h_{fg}$ then the bulk phase energy equation can be written as

$$G_\ell \nabla h_\ell = 4q_{out}/D$$

but if $q_{out} \longrightarrow 0$ for $T_\ell \longrightarrow T_s$ then either $G_\ell$ or $\nabla h_\ell \longrightarrow 0$ and we have the above delemma.*

Superheating of the Liquid

If the bulk phase is allowed to superheat then the derivation of $\dot{\Gamma}_{g\ell}$ implies that for $T_\ell > T_s$ $h_{fg}(1 + \beta) \longrightarrow h_{g\ell}$ with $h_\ell > h_s$ and that condensation ceases ($h_A \longrightarrow 0$). In this case

$$q''_{out} = \frac{h_D}{2}(T_w - T_s) + h_D(T_s - T_\ell) \qquad (E\text{-}2)$$

and the maximum degree of superheat (occuring at $G_\ell = 0$) is

$$T_\ell - T_s = \tfrac{1}{2}(T_w - T_s) \qquad (E\text{-}3)$$

This result is unacceptable since $T_w - T_s$ can easily reach 20 - 40° F and $\longrightarrow \infty$ as $\sqrt{q''/h_B^o}$ and bulk superheats will hardly exceed a (very) few tenths of a degree. The phenomenon we have not introduced is the evaporation (or flashing) that will occur. Indeed since $\alpha$ is already generally large (in most cases) when $T_\ell \longrightarrow T_s$ there will be a fairly large surface area for the superheated liquid to evaporate across.

---

* There is a mathematical out, if $q_{out} \propto (T_s - T_\ell)^a$ with $0 < a < 1$ then $T_\ell \longrightarrow T_s$ at a finite value of Z. Indeed if $G_\ell$ does not change much $Z_s = \dfrac{\left(T_s - T_\ell(o)\right)^a \; C_p G_\ell}{(1 - a)C}$ with C a proportionality constant. There is no evidence that a is < 1 indeed there is much to say it is $\geq 1$.

In a given volume the amount of additional voidage created by the superheated liquid is

$$\Delta\alpha = (1 - \alpha)\, \rho_\ell\, (h_\ell - h_s)\, /\rho_g\, (h_g - h_\ell). \tag{E-5}$$

we propose that the rate of evaporation is proportional to

$$(\Delta\alpha)\, \rho_g v_g = (\Delta\alpha)\, \rho_g S v_\ell$$

hence for $T_\ell > T_s$

$$\dot{\Gamma}_{g\ell} \longrightarrow 4\, (q'' - q''_{out} + C_E \Delta\alpha \rho_g v_g h_{g\ell})/h_{g\ell} D_e \tag{E-6}$$

This leads to a maximum superheat of

$$T_\ell - T_s = \tfrac{1}{2}\, (T_w - T_s)/(1 + C_E G_\ell Sc_p/h_D) \tag{E-7}$$

and eqs(E-4,5,6) imply that the evaporation Nussult number is

$$Nu)_E = C_E S Pe_\ell \tag{E-8}$$

Analysis of E-7 shows that the superheat still $\longrightarrow \infty$ with $\sqrt{q''}$. Quantification however shows that even for $q'' \approx 10^7$ B/hr ft.$^2$ where $T_w - T_s \approx 200^\circ$F we find for small Pe number ( $\approx 1000$) that a value of $C_E \approx 1$ keeps the superheat below $\tfrac{1}{2}^\circ$F. For reasonable values of q" and Pe a value of $C_E \simeq 0.05$ is sufficiently large and we use this value in the model. It should be stated that we have not been able to find experimental data to support this approach to bulk evaporation and while the steady state void fraction and wall temperatures are not meaningfully affected by the choice of $C_E$ it is not clear how transient calculations will be affected. Such studies will be performed in the future.

It is clear that as the heated length is extended beyond the location of saturation (i.e., into very high void fraction) that the vapor will start to superheat. This effect will alter the form of $\Gamma_g$. We do not consider this phenomenon at this time.